Pedro Miguel Courelas Peres

Licenciado em Ciências da Engenharia Eletrotécnica e de Computadores

Switched Reluctance Motor Fault Tolerant Operation

Dissertação para obtenção do Grau de Mestre em

Engenharia Eletrotécnica e de Computadores

Orientador: João Francisco Alves Martins, Professor Associado, FCT/UNL

Co-orientador: Vítor Manuel de Carvalho Fernão Pires, Professor Co-ordenador, Instituto Politécnico de Setúbal

Júri

Presidente: Prof. Doutor Rui Alexandre Nunes Neves da Silva
Arguente: Prof. Doutor Armando José Leitão Cordeiro
Vogal: Prof. Doutor João Francisco Alves Martins

FACULDADE DE CIÊNCIAS E TECNOLOGIA
UNIVERSIDADE NOVA DE LISBOA

Dezembro, 2019

Switched Reluctance Motor Fault Tolerant Operation

Este documento foi gerado utilizando o processador (pdf)LaTeX, com base no template "novathesis" [1] desenvolvido no Dep. Informática da FCT-NOVA [2].
[1] https://github.com/joaomlourenco/novathesis [2] http://www.di.fct.unl.pt

To my family...

Acknowledgements

First I would like to give a big thank you to my adviser, professor João Martins, for all his support, patience and time in helping me with my dissertation. Without his help this project and subsequent paper wouldn't be possible.

I would also like to thank professor Vitor Pires from Polytechnic Institute of Setúbal for his hints in some aspects of the project.

I also would like to thank the institution where this work was developed, the Electrical and Computer Engineering Department of FCT/NOVA. I give my thanks for the support and resources that they have lend me.

Finally I want to give a big thank you to my family and friends for all their support on this long and difficult year. They are the ones who gave me strength to go on and face the challenges that this journey has given me.

Abstract

In recent years, with the development of micro and power electronics, the switched reluctance machine has been gaining popularity. This type of machine is attractive because it has a cheap and easy construction, having absence of rotor windings and permanent magnets. It has also an inherent fault tolerance ability.

Due to this fault tolerance it has gained the attention of industries and applications that require safe and reliable operation. However, the machine is only fault tolerant to a point and, with the aim of improving its already high fault tolerance, multiple studies were conducted on the subject.

In this dissertation a new passive fault tolerant method, comprising on simple modifications in the windings, converter and control method will be presented. Worth notice that one of the modifications is already discussed in the cited literature. This method is aimed principally at open circuit faults in the windings with the machine working as a motor in the low speed zone.

The effectiveness of this method will be studied by comparison of a regular SRM with one with the solution through simulation of winding fault conditions, namely open and short circuits faults. In order to do this, first finite element analysis was performed, with the software *Flux2D*®, in order to obtain the magnetic and torque characteristics of the machines. This was followed by dynamic simulations in *Matlab-simulink*®. It will be shown that the method is very effective for open circuit faults but will only have negligible improvements in case of winding short circuits.

Keywords: Switched reluctance motor, SRM, fault tolerance, finite element analysis, winding open circuit fault.

Resumo

Em anos recentes, com o desenvolvimento da microeletrónica e da eletrónica de potência, a máquina de relutância comutada tem ganho popularidade. Este tipo de máquina é atrativo porque tem uma construção barata e fácil, não tendo enrolamentos no rotor nem magnetos permanentes. Outra das razões importantes é devido a ter uma tolerância a falhas característica.

Devido a esta tolerância a falhas ganhou a atenção de industrias e aplicações que requerem operações seguras e fiáveis. No entanto, a máquina é tolerante a falhas apenas até um certo ponto e, com o intuito de aprimorar esta característica, vários estudos foram desenvolvidos sobre este assunto.

Com esta dissertação pretende-se introduzir um método tolerante falhas envolvendo pequenas modificações a nível da sua arquitetura, conversor e controlo. Importante referir que uma destas modificações já se encontra presente na literatura citada. Este método é apontado diretamente a falhas de circuito aberto nos enrolamentos da máquina com esta a funcionar na zona de velocidade baixa.

A eficácia deste método vai ser estudada por comparação, através de simulação, de uma máquina normal com a máquina com a solução em caso de falhas nos enrolementos, nomeadamente curto circuito e circuito aberto. Para isto foram primeiro obtidas as características magnéticas e de binário através do Método dos Elementos Finitos das máquinas, com recurso ao software *Flux2D*®, procedendo-se depois à sua simulação dinâmica em ambiente *Matlab-Simulink*®. Vai ser mostrado que a máquina com solução é eficaz em casos de circuito aberto, mas em curto-circuito de enrolamentos as melhoras são quase inexistentes.

Palavras-chave: Motor de relutância comutada, SRM, tolerância a falhas, método dos elementos finitos, circuito aberto nos enrolamentos.

Contents

List of Figures

List of Tables

Acronyms

CHC	Current hysteresis control/controller
emf	Electromotive force
FEA	Finite element analysis
PI	Propotional Integral Controller/control
RPM	Revolutions per minute
SRM	Switched Reluctance Machine

Symbols

P_{elec}	Electrical power
i	Varying current
J	Moment of inertia
k	Attrition coefficient
L	Self Inductance
M	Mutual Inductance
ψ	Varying linkage flux
Ψ	Linkage flux characteristics
R	Electrical resistance
t	Time
T	Period of time
θ	Rotor position
Γ	Torque
Γ_{rpp}	Torque ripple
u	Varying voltage
V	Voltage
ω	Angular Velocity
W_{mag}	Magnetic energy

W'_{mag}	Magnetic co-energy	*

CHAPTER 1

INTRODUCTION

1.1 Motivation

The switched reluctance machine is known for its inherent fault tolerance, cheap construction, absence of winding in the rotor and absence of permanent magnets[1][2].

Due to this characteristics and the crescent development and better availability of microprocessors and power electronics drives, in recent years it has been attracting for itself a large investigation in distinct fields[3][4]. It also makes the machine a fine choice for a wide range of applications that require safe and highly reliable operation, such as a aircraft operation, automobile applications and many others [5].

Such requirements justify the investigation done in the field of improving its already high fault tolerant abilities in order to make it even more reliable in the presence of faults.

The investigation on the SRM is a great deal done for its control and behavior in the presence of faults. There is already a wide range of investigation done on fault modeling, fault detection and construction techniques to improve the machine fault tolerance. However it is never to much to add new findings to increase the database of possible methods and constructions.

1.2 Objectives

In this dissertation it is pretended to introduce a new fault tolerant method for the SRM and analyze it for winding faults. The method consists in a modification of the windings, converter and control of the machine, being the winding modification already presented in literature.

The evaluation will be done by simulation. The machine will be modeled for the normal and proposed solution constructions and simulated in winding fault conditions.

The results will be discussed and compared.

The modeling will be first in *Flux2D*® for magneto-static simulations. Their purpose will be to obtain the flux and torque characteristics of the machine through finite element analysis. This characteristics will then be used in a *simulink*® model in order to perform dynamic simulations.

1.3 Structure of the document

This dissertation is divided in six chapters being the first chapter this introduction.

The second chapter consists in the state of the art about the SRM. It will first introduce the concepts of the machine followed by an introduction to the common faults, in windings and converter. Finally the most interesting fault tolerant approaches in literature will be presented in the final section of the chapter.

In the third chapter the normal machine, i.e. the machine without the solution, will be presented and its modeling will be shown and explained. Finally it will be simulated in a start condition and in a steady state condition.

The fourth chapter will firstly present the normal machine in winding fault conditions. This will be followed by the proposed solution and its modeling. The chapter will finish with the presentation of the simulation results of the solution machine in a start and steady state conditions, comparing them with the ones from the normal machine.

In the fifth chapter the simulation results for the proposed solution in faulty cases will be presented, analyzed and compared with the faulty ones from the normal machine.

In chapter six the final conclusions and future possible work will be discussed.

Chapter 2

Introduction to the machine and state of the art

2.1 Ideal characteristics of the machine

2.1.1 The switched reluctance machine

The switched reluctance machine is probably the simplest type of electrical machine [6]. It is formed of a stator with magnetization poles and a salient pole rotor with no windings. In figure 2.1 it is represented a cross section of the machine with 8/6 pole configuration (8 in the stator, 6 in the rotor).

This type of machine started to become popular with the power and micro electronic revolutions, necessary for its control[6].

Its operation resides in the principles of electromechanic energy transformation. Being the rotor free to rotate and existing a magnetization source, the magnetic circuit of the machine will tend to get to the position of least reluctance and higher inductance. This can be described mathematically starting by expression 2.1:

$$\Gamma_r = -\frac{\partial W_{mag}}{\partial \theta} = \frac{\partial W'_{mag}}{\partial \theta} \tag{2.1}$$

Where Γ_r is the torque supplied from the system to the rotor and W'_{mag} is the magnetic co-energy present in the coils. It is important to note that the first derivation should be done at constant flux and the second at constant current.

In the SRM the inductance of each one of the coils will vary between a lower value, when the stator pole is completely unaligned with a rotor pole, and a higher value when it is completely aligned[6]. This means that the inductance of a phase will depend on the rotor position θ in relation to it. With this dependence in mind, in the case of figure 2.1,

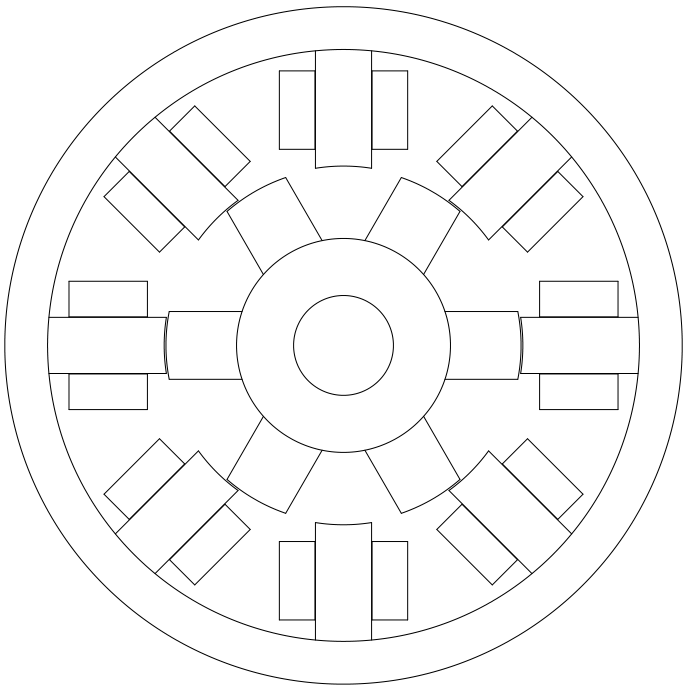

Figure 2.1: Drawing of a cross section of a switched reluctance machine.

and assuming a linear magnetic material, the magnetic co-energy can be expressed as:

$$W'_{mag} = \frac{1}{2}\sum_{i=1}^{4} L_i(\theta) i_i^2 + \sum_{i=1}^{4}\sum_{j=1}^{4} M_{ij}(\theta) i_i i_j \tag{2.2}$$

Applying to 2.2 the expression 2.1 the following relationship is obtained:

$$\Gamma_r = \frac{1}{2}\sum_{i=1}^{4} \frac{dL_i(\theta)}{d\theta} i_i^2 + \sum_{i=1}^{4}\sum_{j=1}^{4} \frac{dM_{ij}(\theta)}{d\theta} i_i i_j \tag{2.3}$$

In the SRM it is also possible to do an approximation and neglect the mutual inductances coefficients [6]. So 2.3 can be simplified to:

$$\Gamma_r = \frac{1}{2} i_1^2 \frac{dL_{11}(\theta)}{d\theta} + \frac{1}{2} i_2^2 \frac{dL_{22}(\theta)}{d\theta} + \frac{1}{2} i_3^2 \frac{dL_{33}(\theta)}{d\theta} + \frac{1}{2} i_4^2 \frac{dL_{44}(\theta)}{d\theta} \tag{2.4}$$

In figure 2.2 the ideal desired curves of the inductance and torque are represented for an 8/6 machine with stator pole angle of 18º and rotor pole angle of 22º. Although the curves were obtained for an ideal machine, they serve to illustrate its functioning. Because torque depends on the square of the current its sign only takes into account the derivative of the inductance and not on the current sign. This can be observed in figure 2.2 and in equation 2.4.

The curves in figure 2.2 were obtained at constant current, however, during the operation the current should, ideally, only be constant at the intervals that suit its work. This means that for motoring the current should ideally be constant (and $\neq 0$) in the increasing inductance zone[6] [7]. On the other hand, the machine in order to work as a generator

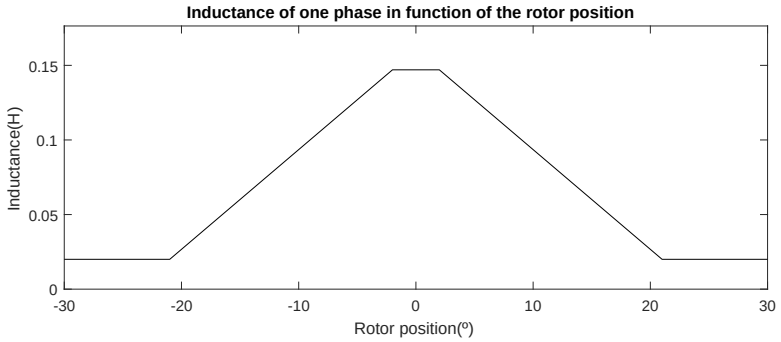

(a) Inductance of one phase of one switched reluctance machine.

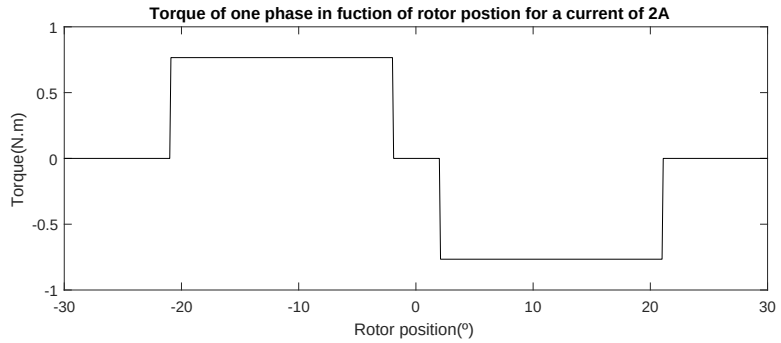

(b) Torque characteristic of one phase in function of rotor position.

Figure 2.2: Torque and inductance curves for one phase of a SRM.

the opposite would be wanted since, as in all electrical machines, the switched reluctance generator is the dual of the motor [8] [9].

2.1.2 Converter

In the SRM various possible converter circuits exist. While some can be used with most loads, a large part are better suited only for specific niche applications but being most cost effective in that niche [10]. However, for the studied machine a traditional asymmetric bridge converter was chosen. The converter is represented in figure 2.3. The reasons for choosing this converter were its simplicity and because it is often found in the cited literature.

This converter has a simple working principle. When the switches are turned on the load will be supplied by the source. If the load is inductive when the switches turn off the current still present in the inductor will be sent to the source by the diodes.

A functionality of the half-bridge converter which is important to the SRM is the ability (with the proper switch control) to perform current hysteresis control. If, during conduction time, one of the switches turns on and off when the current value passes trough certain values ($I_{avg} \pm Hysterisis\ threshold$) it will keep an average value equal to the one desired.

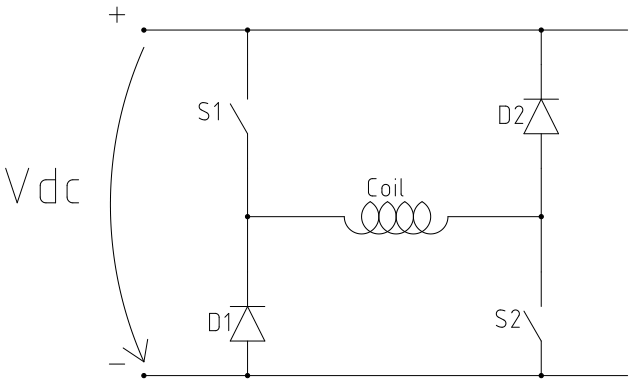

Figure 2.3: Asymmetric bridge converter.

2.2 Faults

The study of faults, fault detection and implementation of new fault tolerant methods in the SRM has been a topic of interest for many investigators.

According with [4], the faults of the machine can be subdivided in two main groups: internal and external. The internal faults include all that occur in elements of the machine. Some examples include a broken winding, partial and total short-circuits, phase to phase faults and eccentricities of the rotor. The external faults include all that do not occur in elements of the machine. Some examples include converter faults, voltage supply faults and load faults.

2.2.1 Open circuit fault on a coil

The first fault that will be studied is the open circuit on a coil. This type of fault will provoke a loss on the average torque, typically proportional to the number of phases that got disconnected [11], [12].

If the machine has each pole connected separatly (i.e. each stator pole is a phase) in case of a fault unbalanced forces will appear on the rotor (due to flux imbalances) [13], potentially being dangerous to the machine.

It is reported in [14] that either with the machine with no load or with its nominal load that it can continue working with its nominal speed. However it will have larger currents in the healthy phases and an increase on velocity and torque ripples. This effects are more accentuated the closer to the nominal load.

2.2.2 Coil short circuit

In the coil faults we still have the short-circuits. This faults include partial short-circuits (some turns), total short-circuits(whole coil), phase to phase and phase to ground.

The case of a partial short-circuit is studied in [15] with machine already in its steady state. Is shown by simulation and by experiments that if the machine is in current hysteresis control, the controller will keep the current with its nominal value but a reduction of the torque supplied by the faulty phase will happen. It is shown in the same article that in voltage control mode, current spikes will appear in the beginning and end of each conduction period. The latter are smaller the higher the speed of the machine.

It is shown in [13] that a partial short circuit can induce unbalanced lateral forces in the machine.

It is also shown in [12], that in a partial short-circuit it is still possible to salvage some torque of the affected phase but with less efficiency. Nevertheless, according to the author, can be justifiable in certain cases.

The case for a total coil short-circuit is presented in [13] during the acceleration of the machine. It is shown that when a total short-circuit occurs that the phase is isolated from the demagnetizing voltage. If it occurs when the coil is conducting non controlled pulses will appear in the shorted phase due to it entering the generation region and not be able to demagnetize itself. This pulses will continue until there is no energy left in the phase and will tend to zero in some revolutions. In [12] is shown that for a complete short-circuit no torque can be salvaged from the phase.

2.2.3 Short circuit between two phases

Phase to phase faults occur when two conductors of adjacent phases come into contact. This fault is studied will great detail in [2]. Besides the article not being dedicated to the fault a detailed mathematical model is presented with an explanation for a large number of possible outcomes. According to [11], this fault will provoke over-currents and an increase on the vibration of the machine but will not cause significant loss in torque.

2.2.4 Phase to ground fault

The phase to ground faults occur when a conductor has a conduction path to neutral. This case is studied in [12]. When this fault happens the path that is shorted will barely conduct while the short will bypass any diodes and switches. In the short path a current will appear because of the varying flux in the turns. If the short does not occur in the upper half (i.e. it does not bypass the transistor and diode connected to the source) still some torque can be produced by the phase [12].

In [11] is pointed that if the current sensing is done outside the short-circuit path (the bypassed zone), a wrong current reading will be done. This can potentially provoke a large over-current with possible devastating effects.

2.2.5 Rotor Eccentricities

Eccentricities in the rotor are also a topic of interest. According to [16] there are three types of eccentricities: Static eccentricity(SE), Dynamic eccentricity(DE), and Mixed eccentricity(ME).

The static eccentricity is a translation of the rotation axis in which the axis remains static but the air gap is reduced in the faulty pole[16].

In the dynamic eccentricity the center of the rotor is not the rotation axis. This will make the minimal air gap to rotate with the rotor [17].

In the mixed eccentricity, as the name indicates, the effect provoked in the air gap will be a junction of the previous two [16].

The way eccentricities affect the machine depend on its geometry. In some cases a small increase in torque is reported [18] while in others no noticeable changes were found regarding the torque [19]. However, eccentricities always induce unbalanced forces in the rotor [18] [19]. In [19] is reported a pulsating force that generally has the direction of the least air gap. A similar result had been previously reported in [18].

2.2.6 Short-circuit in a switch

A short circuit in a switch is a fault that will provoke a current with excessive amplitude that can even disconnect the affected phase if it has over-current protection. If this is the case then the fault will do the same effect as an open-circuit fault since it is disconnected from the source [20].

During the transient of the speed, an short-circuit in the converter can be dangerous because of the rapid variations of the torque [20].

2.2.7 Open circuit in a switch

In the case of an open circuit in a switch the effect will be the same as if it was an open circuit in a winding [11]. If the converter is the asymmetric bridge it does not matter which of the transistors has the fault since with only one the phase is not able to magnetize itself [21].

This fault will provoke a loss in speed due to the reduction of the average torque but this can be compensated by the healthy phases. The effect is involuntary if the machine is in voltage control mode [20].

2.2.8 Voltage source faults

The voltage source faults were analyzed in [14]. In the article the first case studied is a drop of 33% on the DC link voltage. This could be provoked by a fault in a rectifier bridge. It is demonstrated that this will not affect the velocity if it is below its nominal load. If it higher it will settle in progressive smaller speed values. As the voltage gets lower the machine compensates this by increasing the current.

Still in [14] it is studied a second case where the voltage supply is temporarily turned off. In the exact moment of turning it off the DC link voltage as an exponential decay until zero. When is turn on again, the DC link will have an exponential increase until it reaches the source voltage. During both transients, the speed will have a drop during the turned off phase and will rise again when it is again turned on. The current and torque will also have a drop during the source turned off but will have spikes the moment when it is turned on. After both transients the machine continues to work normally.

2.3 Fault tolerant methods

Before fault tolerance be discussed, a mention should be made to fault detection. Fault detection, although not always required, it is essential to some fault tolerant methods. In [11] it is presented three of the first fault detection methods consisting in a differential current detector, differential flux detector and rise time detector. In [21] a converter fault detection method is proposed based on the difference between the expected and supplied current from source. In [16] a fault detection method based on differential high frequency current pulses signatures is presented for eccentricity detection. In [22] a new a new machine architecture is presented with inherent fault detection abilities.

In terms of fault tolerance, practically all literature cited mentions that the machine has this characteristic intrinsically. The first methods of fault tolerance were based on disconnecting the faulty phases and let the other phases compensate the lost torque. This could done with control schemes based on PID controllers as stated by Stephens in [11] or with Fuzzy Logic based controllers as stated in [23]. However this is true only to a certain point and even with just one faulty phase the performance lowers. In order to help the machine to have a higher degree of tolerance to faults, several investigators proposed numerous modifications to the machine itself and its converter, as well its control scheme. In this section some of this modifications and methods are mentioned.

Several fault tolerant methods consist solely on modifications of the converter. In [24] several mechanic switches are introduced to the Half-Bridge converter connecting two different phases. The purpose is to supply the affected phase by a healthy one who does not share the same conduction time. In [25] is presented a converter based in Neutral Point Clamping Inverters, where the normal destructive states are used in this case to bypass faulty switches. Still for fault tolerance in converters, in [26] it is proposed a Full Bridge Inverter divided in four parts, each one connected to a relay. The fault tolerance resides, for open circuit faults, in the possibility for bidirectional currents, which will let, in a case of a open circuit, to use the opposite side of conduction to secure the machine's operation. For the case of short-circuits, the relay of the affected part will open the connection with the voltage source. This combined with a special control strategy for short-circuit faults will secure the machine's operation.

Solutions based on the modification of the machine are also possible. In [13] several rearrangements of the machine windings with different fault tolerance capabilities are

presented. Worth to notice that one of them is used, in combination with other methods, as a part of this dissertation solution. In [27] is presented a double redundancy switched reluctance machine where each phase is composed by two coils which can be controlled separately. In [28] it is proposed a fault tolerant construction based on short flux paths by having higher number of rotor poles than stator poles.

There are also alternative solutions that can mix various type of machine changes. In [2] a fault tolerant method exclusively for phase to phase faults is presented. This method consists in a special fault detection method with a triple closed loop control scheme designed exclusively to mitigate currents between phases. In [3] modular machine with redundant power converter and bio inspired control is presented to increase fault tolerance in the machine, power converter and control scheme alike.

CHAPTER 3

MODELING OF THE MACHINE

3.1 Proposed machine and characteristics obtainment

The machine studied is also of the 8/6 type. Its dimensions are found described in table 3.1. The machine dimensions were based on the ones presented in [29], having as the main difference the number of turns per phase.

Table 3.1: Dimensions of the studied machine.

Aspect	Value	Unit
Number of rotor poles	8	-
Number of stator poles	6	-
External stator diameter	190	mm
Internal stator diameter	166	mm
Internal rotor diammeter	60	mm
Shaft diameter	30	mm
Stator pole height	32.7	mm
Rotor pole height	19.8	mm
Rotor pole arc	22	mm
Stator pole arc	18	mm
Air Gap	0.5	mm
Number of turns per phase	300	turns

To obtain the parameters of the machine it was used the software *Flux2D*® to perform magneto-static simulations. In table 3.2 the properties of the magnetic material for the machine yoke are presented. The $B-H$ curve of the material (figure 3.1) was obtained by the arc whose tangent model and no hysteresis losses were considered.

After the construction of the *Flux2D*® project, it was made a parametric simulation varying the current and rotor position to obtain the characteristics of the machine. The

Properties	Value	Unit
Density	7874	kg/m^3
Relative magnetic permeability	1200	-
Saturation Induction Field	1.5	T

Table 3.2: Properties of the material used in the *Flux2D*® simulations.

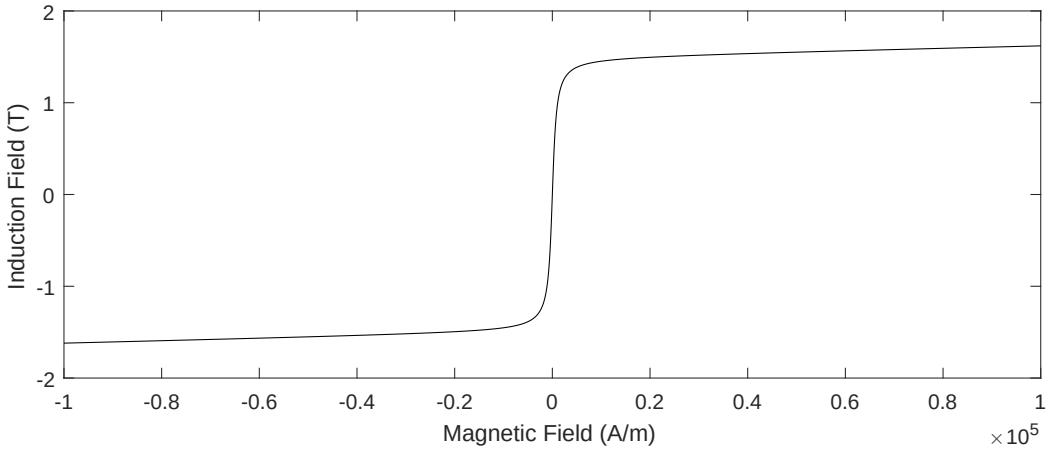

Figure 3.1: B-H curve of the chosen magnetic material.

current varied from -10 A to 10 A with increments of 1 A. The rotor position varied from $-30°$ to $30°$ with increments of $1°$.

The obtained parameters were flux surfaces $\Psi(i,\theta)$ (figure 3.2a) and the torque $\Gamma(i,\theta)$ (figure 3.2b) for one of the phases. For the remaining phases, in both flux and torque surfaces, a translation in the rotor position axis should be made.

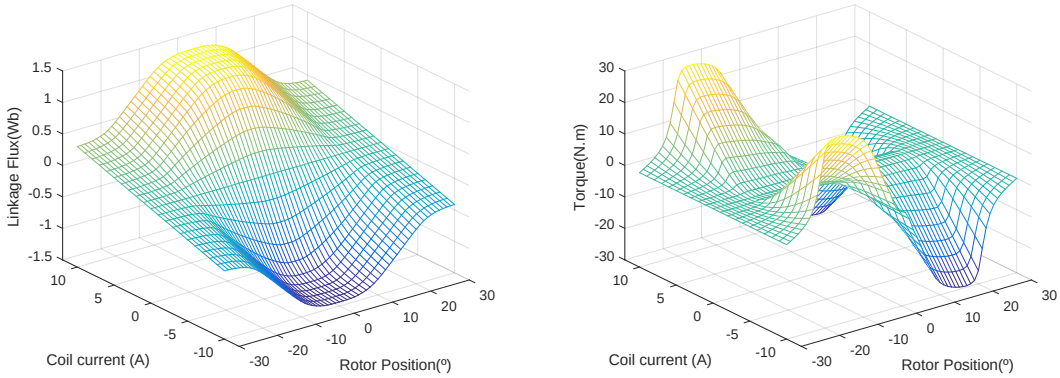

(a) Flux surface of phase 1.

(b) Torque surface of phase 1.

Figure 3.2: Flux and torque surfaces of a machine phase.

However, since it was necessary to simulate short-circuits to analyze the machine, another set of surfaces had to be obtained. The reason for this is the necessity to simulate the winding as two separate ones so that one can be short-circuited in *simulink*®.

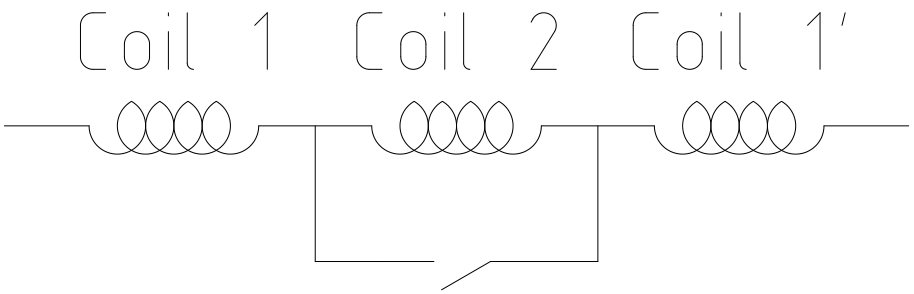

Figure 3.3: Schematic representation of the introduction of the short-circuit fault.

For this the winding was divided in *Flux2D*® as shown in figure 3.3. In the image coil 1 and coil 1' represent one coil and coil 2 represent a second coil, with both having the same number of turns. After the flux project was altered to accommodate this changes new magnetic simulations were performed. Now this simulations will variate two currents (coil 1 current $i1$ and coil 2 current $i2$) and the rotor position θ. Each current and the rotor position will variate with same step of the previous simulation.

With this changes two flux linkages were obtained, coil 1 flux $\Psi 1(i_1, i_2, \theta)$ and coil 2 flux $\Psi 2(i_1, i_2, \theta)$. Together with torque $\Gamma(i_1, i_2, \theta)$ they now depend on three variables.

In figures 3.4a and 3.4b the surfaces of the flux linkage, of coil 1 and coil 2 respectively, are represented for constant and unaligned rotor positions. In figures 3.5a and 3.5b the surfaces of the flux linkage, of coil 1 and coil 2 respectively, are represented for constant and aligned rotor positions. Important to notice that the characteristics are not exactly equal due to the machine construction. In figures 3.6a and 3.6b surfaces of the torque are represented, in function of i_1 and θ, for different coil 2 currents (0 and 10A respectively).

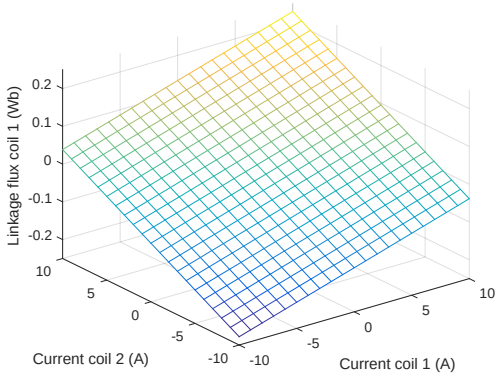

(a) Linkage flux of coil 1.

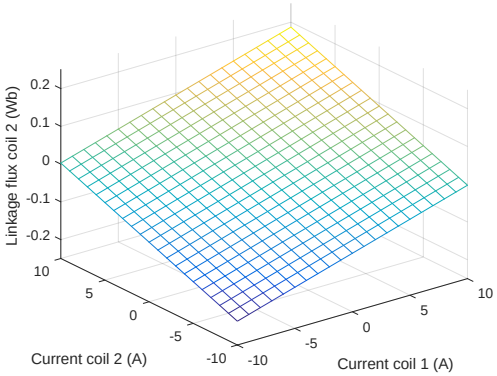

(b) Linkage flux of coil 2.

Figure 3.4: Linkage fluxes of coils 1 and 2 for unaligned position.

3.2 *simulink*® implementation

For the dynamic simulations, the machine was implemented in *simulink*®. In figure 3.7 the main *simulink*® diagram of the project is represented.

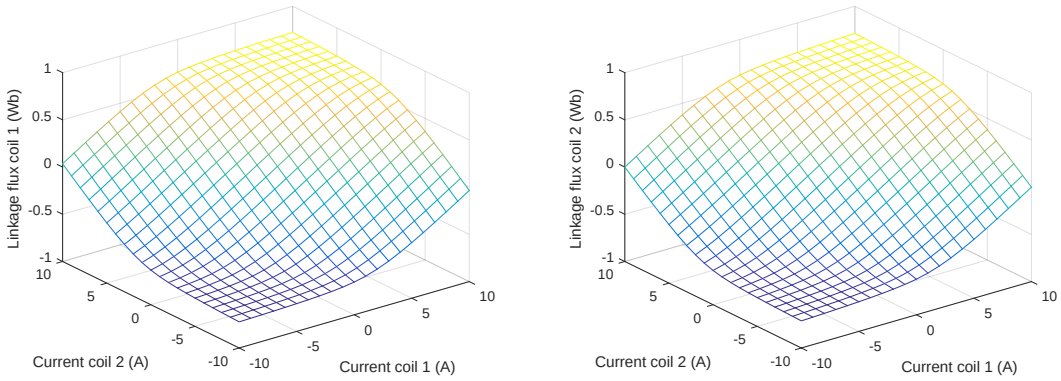

(a) Linkage flux of coil 1 for aligned position. (b) Linkage flux of coil 2 for aligned position.

Figure 3.5: Linkage fluxes of coils 1 and 2 for aligned position.

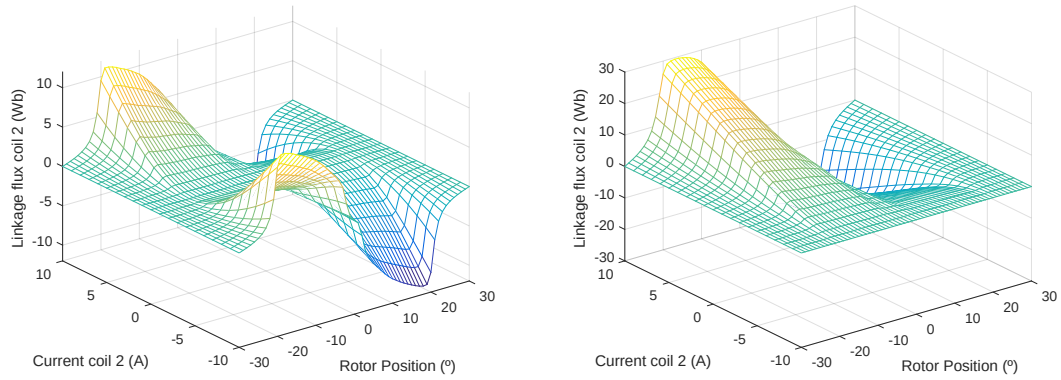

(a) Torque of the full coil with $i_2 = 0A$. (b) Torque of the full coil with $i_2 = 10A$.

Figure 3.6: Torque of the full coil for different currents.

3.2.1 Coil and converter implementation

The implementation of the machine in *Simulink*® was first based on [30]. In the previous article, the machine coils are modulated as current controlled sources, and their current is given by equation 3.1, where V is the voltage at the terminals of the coil, R the resistance of the coil, i_i is the current and L_i is the inductance of fase i.

$$i_i(t) = \frac{\int (V - Ri_i(t))dt}{L_i} \tag{3.1}$$

However, since coils will be connected in series, a new approach was used since current sources should not be connected in series. The approach consists of modeling the coils as voltage sources instead of current sources, as shown in equation 3.2. This method as also the advantage that the inductance and mutual inductance coefficients do not need to be obtained since we have the flux and torque characteristics.

$$emf = \frac{d\psi(i_1, i_2, \theta)}{dt} \tag{3.2}$$

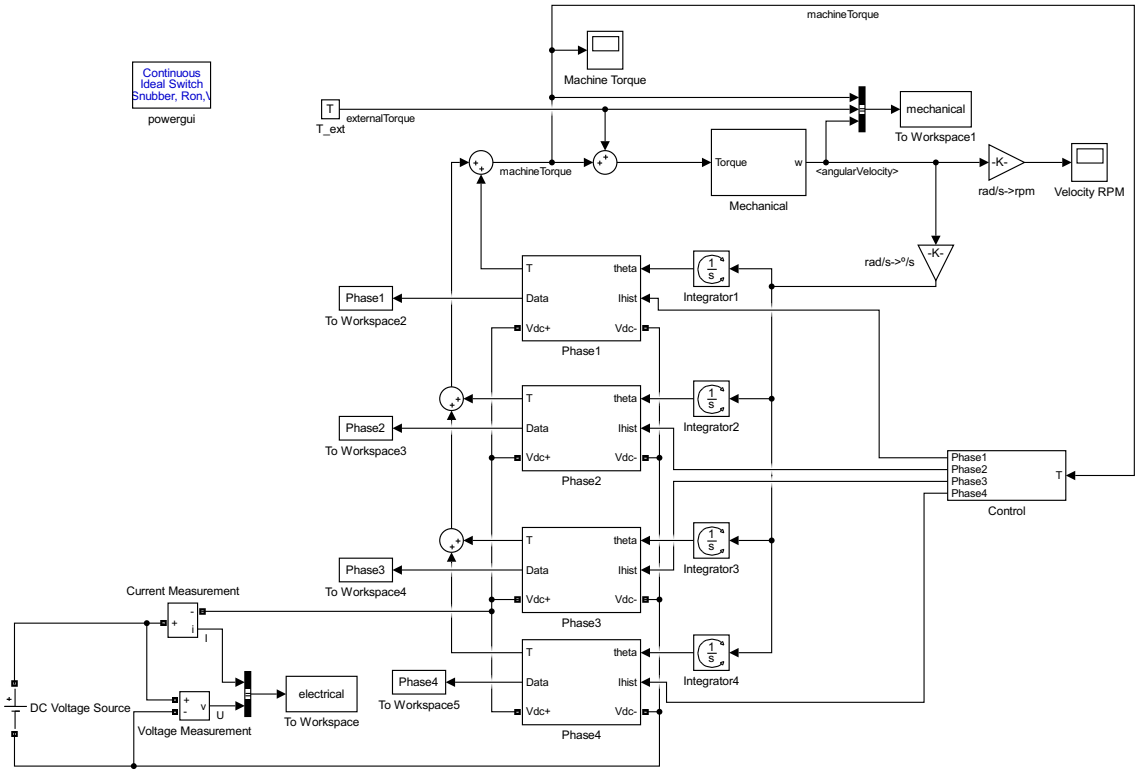

Figure 3.7: *Simulink*® model of the drive.

In the implementation, the package *simscape - power systems* was used for the electrical and electronic simulations. Flux and torque for each phase are implemented by look up tables (two for the fluxes and one for the torque) with the second set of values obtained from *Flux2D*®. In figure 3.8 it is represented the implementation of the electrical model for a phase with fault mechanisms. In the image is seen a series switch at the beginning of the phase. This is to implement an open circuit fault. There is also a parallel switch with the bottom voltage source to implement the winding short-circuit fault.

It should be mentioned that just phase 1 will have the fault mechanisms and the remaining will be normal phases. This phases were implemented with simulation performance in mind. Since they will not have any faults, the flux of the normal phases will only be dependent of one current (equation 3.3). The implementation of this type of phase is represented in figure 3.9. Notice that only one look-up table was used to represent the flux. In this case the first set of values from *Flux2D*® were used.

$$emf = \frac{d\psi(i,\theta)}{dt} \tag{3.3}$$

In figure 3.10 the implementation of the half bridge converter is represented. The phase circuits are supplied by the DC source presented in figure 3.7 with a voltage of $800V$. The phase resistance was set at 2.6 Ω.

Faults will be studied in the next chapter.

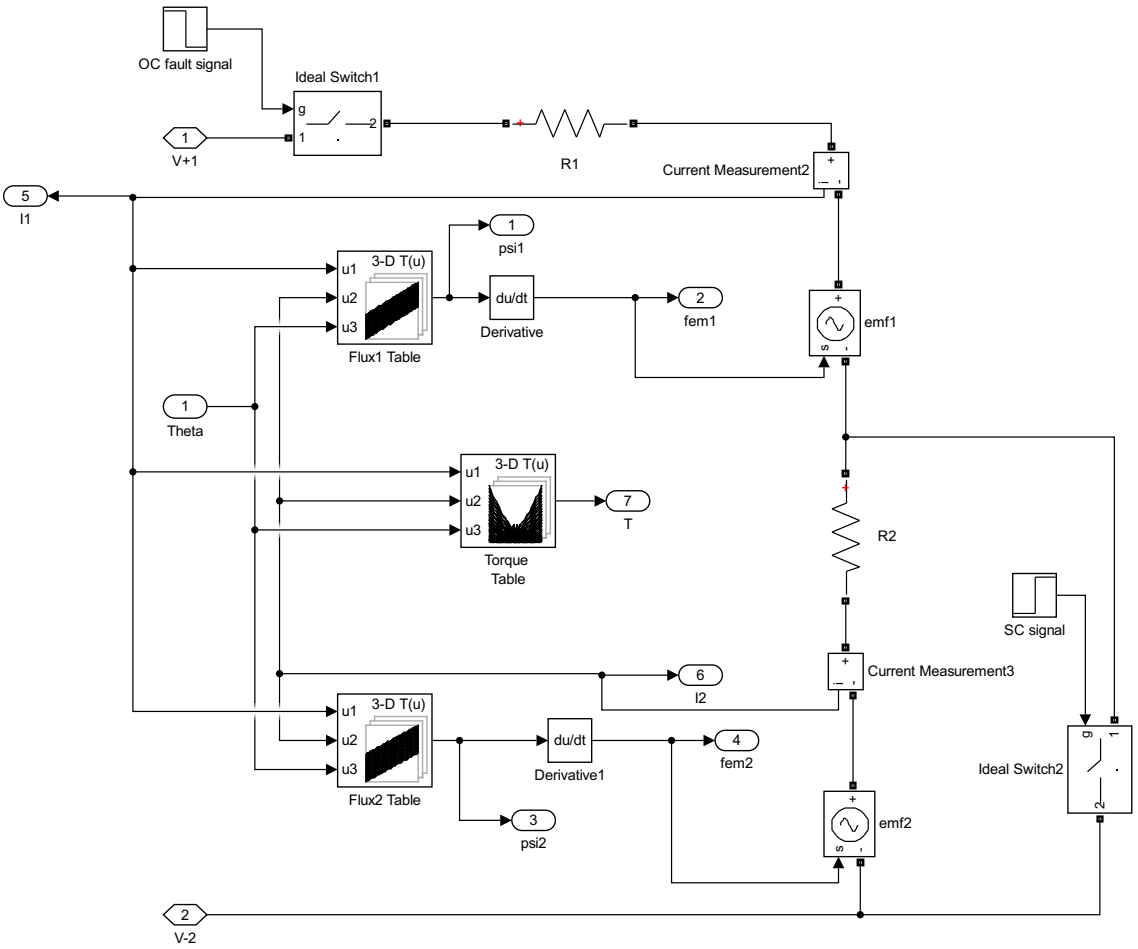

Figure 3.8: *Simulink*® model of the phase with faults.

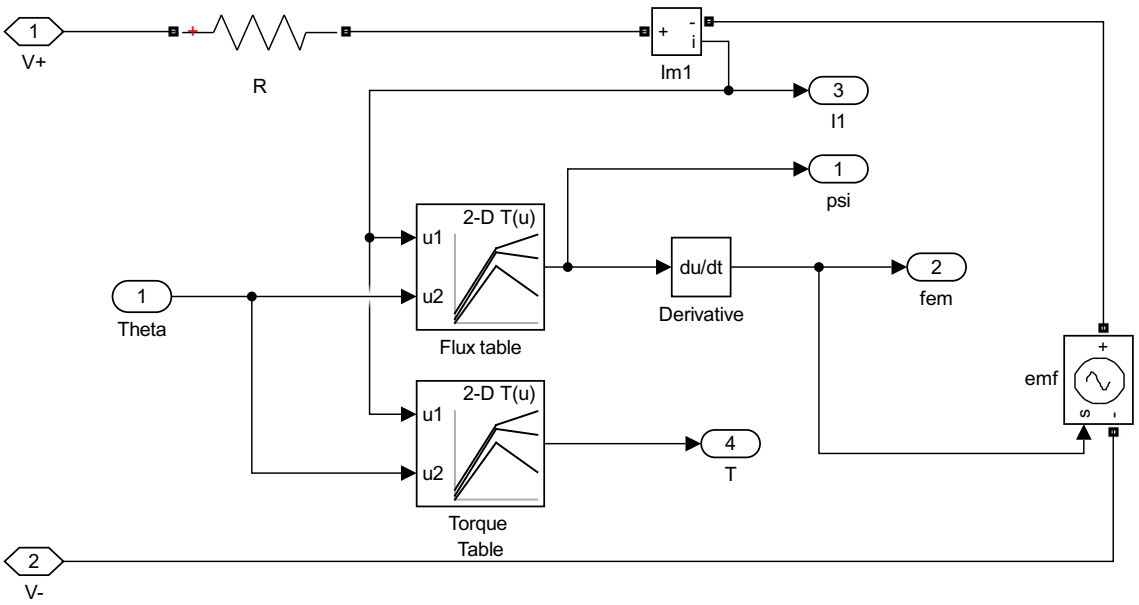

Figure 3.9: Phase implementation on *simulink*®.

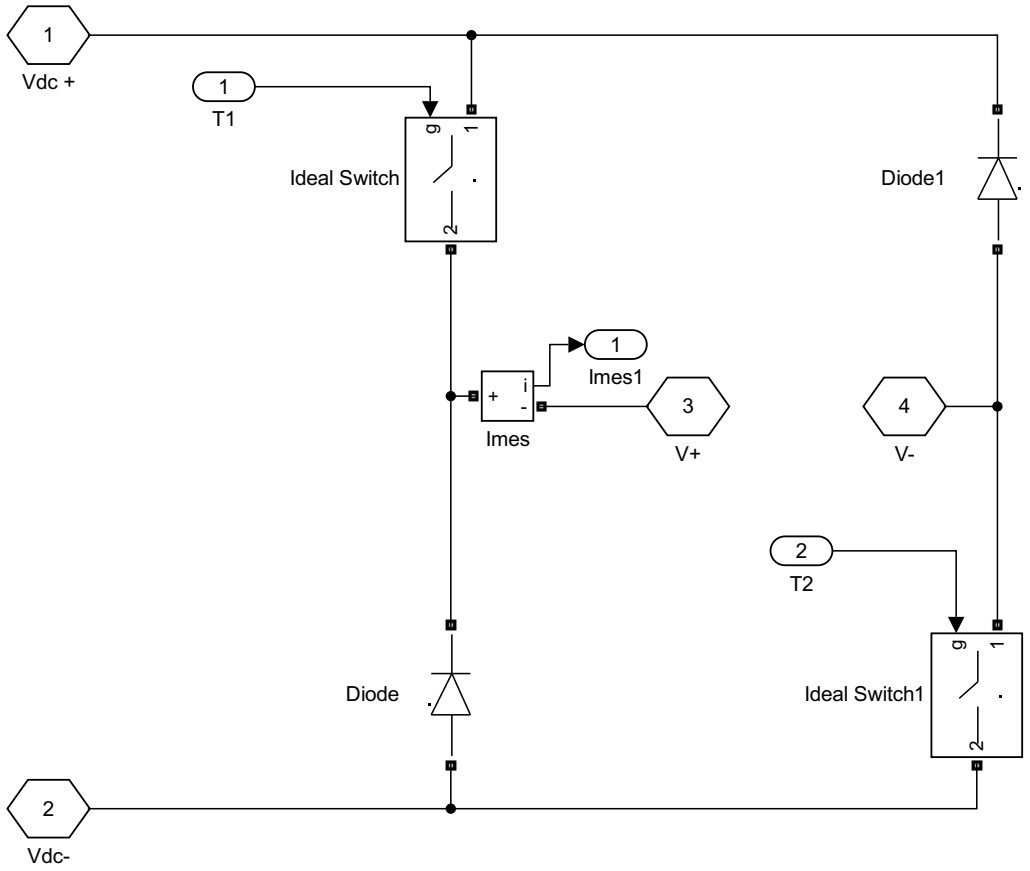

Figure 3.10: Converter implementation on *simulink*®.

3.2.2 Mechanical Implementation

The mechanical modulation is based on the traditional Newton's second law for rolling objects, equation 3.4. Its *simulink*® implementation is represented in figure 3.11. This corresponds to the block mechanical present on top of figure 3.7.

The moment of inertia was calculated recurring to numerical integration and its value is $J = 0.80$ kg/m^2. The dynamic rotation friction coefficient was set to be equal to the one used in [30] with a value of $k = 0.0183$ N.s/m.

$$J\frac{d\omega}{dt} = \Gamma - k\omega \tag{3.4}$$

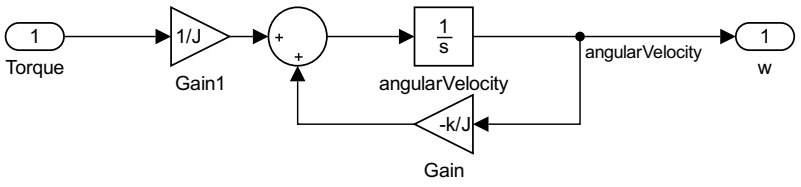

Figure 3.11: Mechanical model implementation.

3.2.3 Control

Two controllers were implemented, a current controller (one for each phase) and a torque controller.

3.2.3.1 Current control

As mentioned before, with the machine working as a motor the coil excitation should be performed when the rotor position is in the increasing interval of the inductance. For that a turn on angle of $\theta_{on} = -23.8°$ was chosen. This is before the rotor being in the increasing inductance interval but gives time for the phase to magnetize before torque production. The turn off angle was chosen to be $\theta_{off} = -8.6°$. This angle is before negative torque production but is needed to give time for the phase to demagnetize before the decreasing inductance region. However, since was not in the scope of this work, it should be mentioned that this angles are not optimized and therefore the torque ripple will present high values.

A current hysteresis controller(CHC) was also implemented together with the on/off control. The hysteresis controller will keep the current between a band of 300 mA around the output of the reference current ($Iref \pm 150$ mA). The implementation of both is represented in figure 3.12.

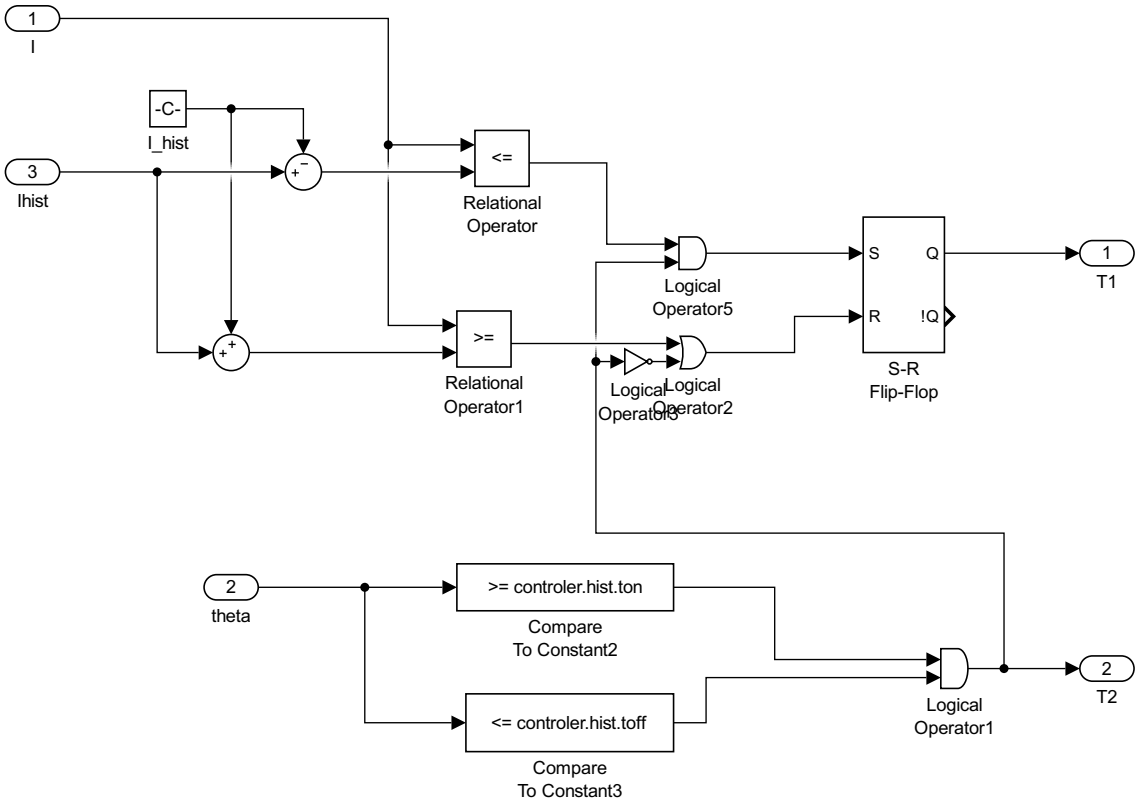

Figure 3.12: *Simulink*® implementation of the current controller.

The bottom part is responsible to detect if the rotor position is in the conducting

interval. If the input position is higher than θ_{on} and lower that θ_{off} the signal of the bottom will be true and enable conduction.

The top part is responsible for the hysteresis. It has two inputs, the top one is the current of the phase and the other is the input reference current. It will check if the current is in the hysteresis band. If true and the phase is in the conduction zone it will keep or change the flip flop state to true. If not, the opposite will be done. Important to note that the flip flop only controls the CHC switch.

3.2.3.2 Torque control

The motor control was implemented with a PI controller in which the control variable is the average torque. This average value is calculated for periods of 50 ms. The output of the controller is a current reference value for the current hysteresis controller. The proportional gain of the PI is $P = 2$ and the integral gain is $I = 0.5$. The PI controller together with the average calculator and reference are represented in figure 3.13. This corresponds to the block 'controler' in figure 3.7.

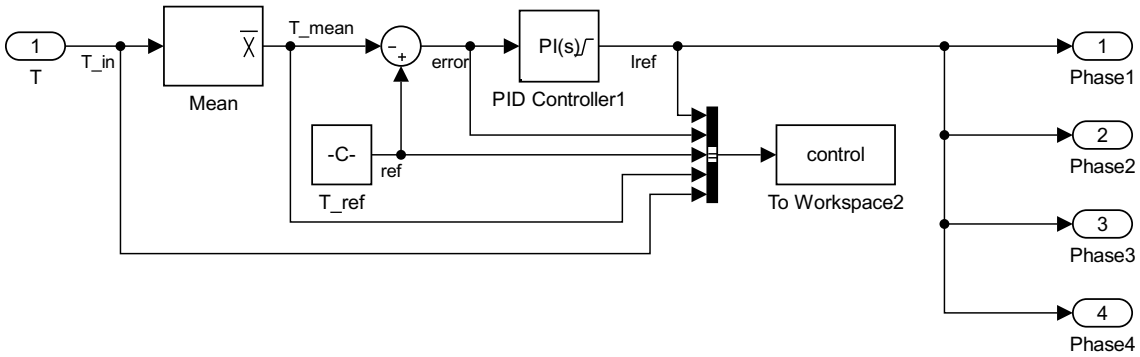

Figure 3.13: *Simulink*® implementation of the motor controller.

3.2.4 Simulation of the motor starting

For demonstration it was performed a simulation of the motor starting until it reached steady state, for a reference torque of 3 N.m. In figure 3.14 it is represented the speed during the entire interval. It can be seen that the motor has a rise time (of the speed) of about 3 s. In figure 3.15 the average torque can be seen.

3.2.5 Simulation of a steady state

In this section a steady state of the normal motor is presented with an average torque of 3 N.m and average speed of 1560 RPM. It will serve for comparison purposes with the faulty cases and the proposed machine solution. In figures 3.16 and 3.17 is represented the machine speed and average torque, respectively.

In figure 3.18 and 3.19 the torque and currents are presented in a smaller time interval. In its center is the time where the faults presented in the next subsections will occur.

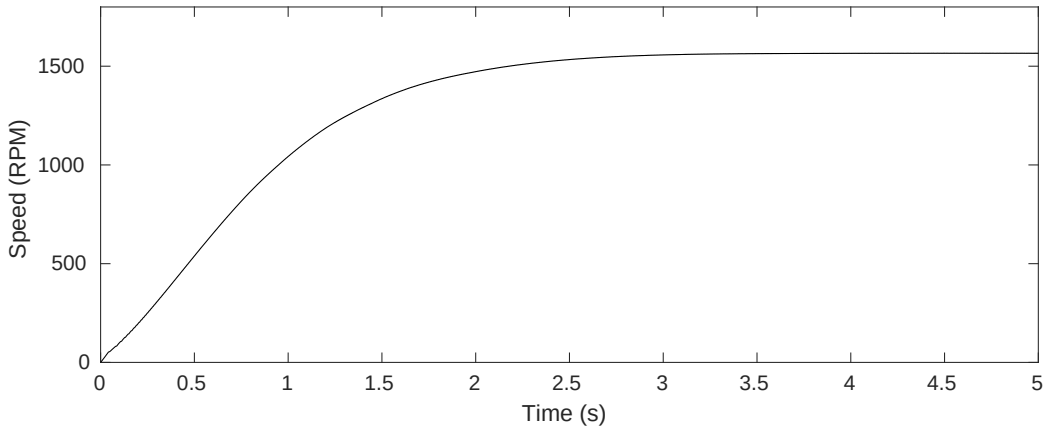

Figure 3.14: Speed of the normal machine during start.

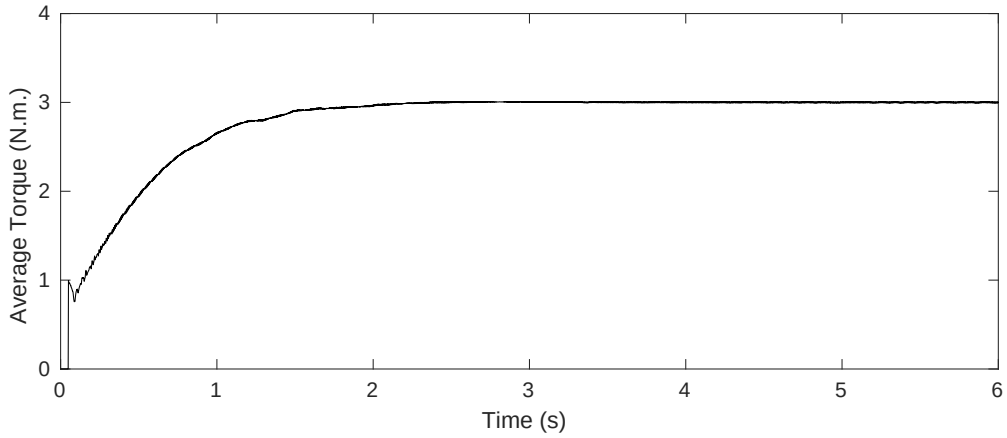

Figure 3.15: Average torque of the normal machine during start.

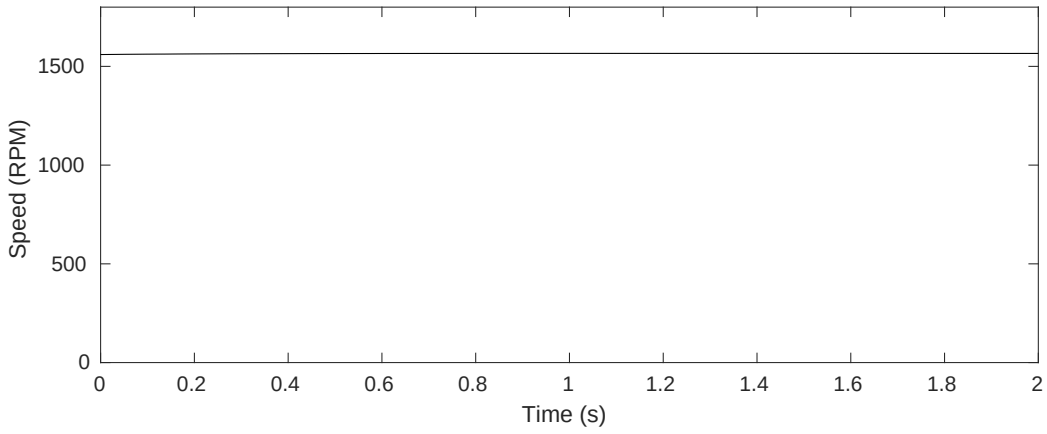

Figure 3.16: Speed of the normal machine in a steady state.

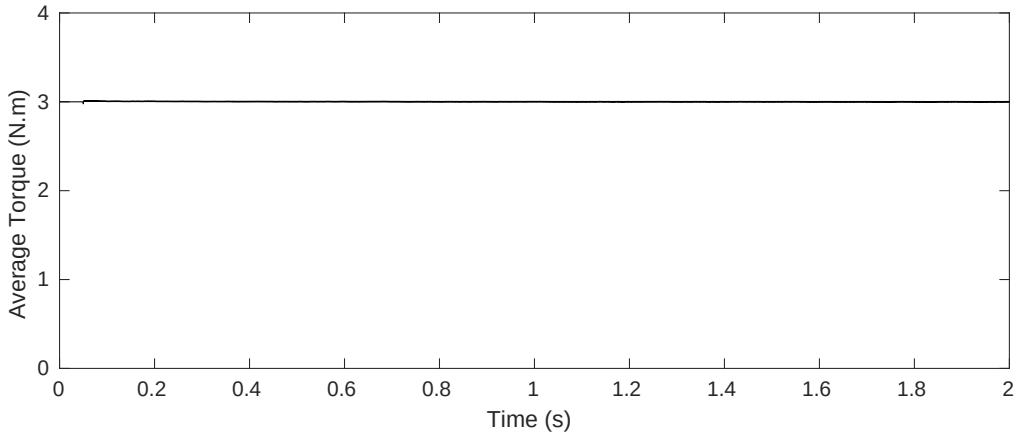

Figure 3.17: Average torque of the normal machine in a steady state.

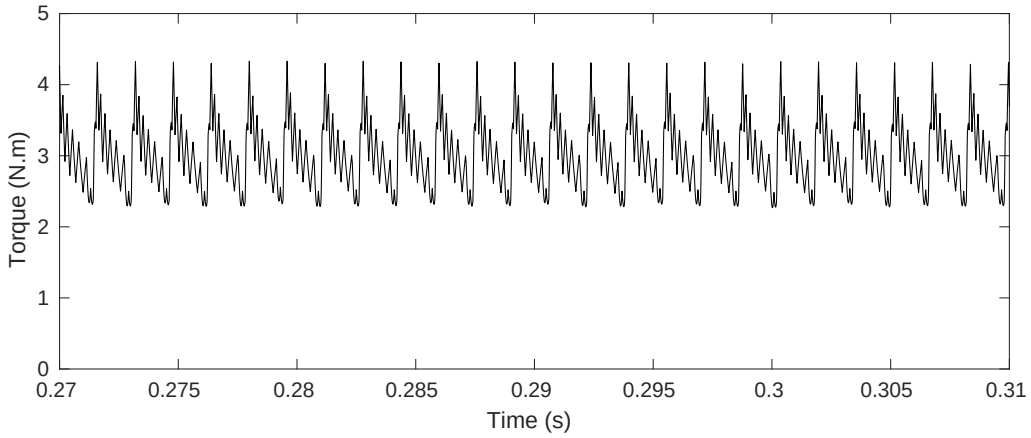

Figure 3.18: Torque of the normal machine in a steady state.

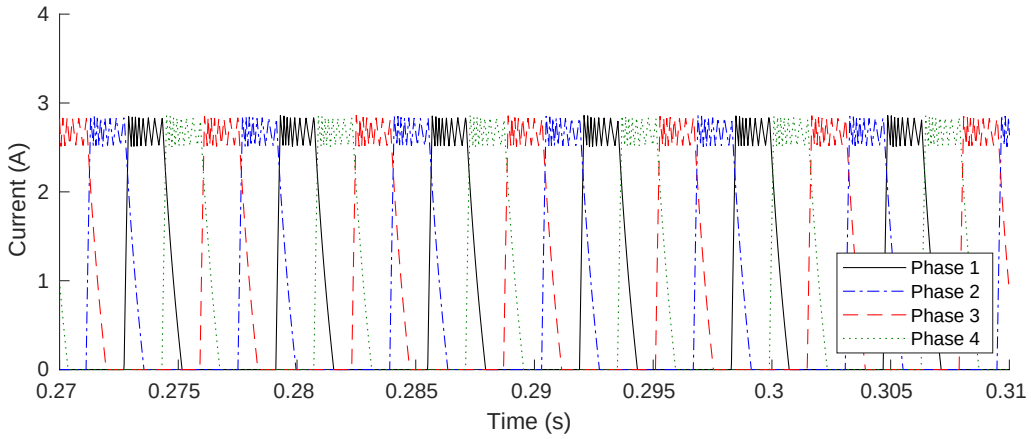

Figure 3.19: Currents of all phases of the normal machine in a steady state.

Besides the waveforms another results are important for comparisons. They are the input electrical power P_{elec} and torque ripple Γ_{rpp}. They are given by equations 3.5 and 3.6 respectively.

$$P_{elec} = \frac{1}{T}\int_0^T u(t)i(t)dt \tag{3.5}$$

$$\Gamma_{rpp} = \frac{\Gamma_{max} - \Gamma_{min}}{\Gamma_{avg}} \times 100 \tag{3.6}$$

This numerical results for the steady state are presented in table 3.3.

Aspect	Value	Units
Torque Ripple	69.7	%
Average Electrical Power	511.5	W

Table 3.3: Results for the steady state of the normal machine.

Chapter 4

Normal machine under fault conditions and proposed solution

4.1 Normal machine under faults

Before the presentation of the proposed solution, the normal machine under faults will be simulated for comparison purposes. To study the motor faults two simulations will be conducted on the normal machine, one under a open circuit and one under a short-circuit. Both faults will be in phase 1 and will be presented with the machine starting in steady state with and average speed of 1565 RPM and a average torque of 3 N.m.

4.1.1 Open Circuit

In this subsection an open circuit fault on the normal machine is presented and analyzed. The fault will occur at the time $t = 0.29$ s. In figures 4.1 and 4.2 the speed and average torque of the machine are presented respectively.

It can be seen that there is a small drop in the speed and average torque, however they will rise back to the in initial values further in time. The drop can be explained by figures 4.3a and 4.3b. In them it can be seen that after the moment of the fault the torque and current pulses from phase 1, the faulty phase, cease to exist.

This will decrease the mean torque by about 25%, however, as already stated in chapter 2, the machine will be able to compensate the torque loss by producing more torque with the healthy phases. This is due to the closed loop torque control where the PI controller will rise the reference current for the current hysteresis to compensate the lost torque. This effect can be visualized in figures 4.3 and 4.4 where it can be noticed that the amplitude of the currents and torque increased further in time after the fault.

Another important detail to mention is the existence of torque dead zones. As seen

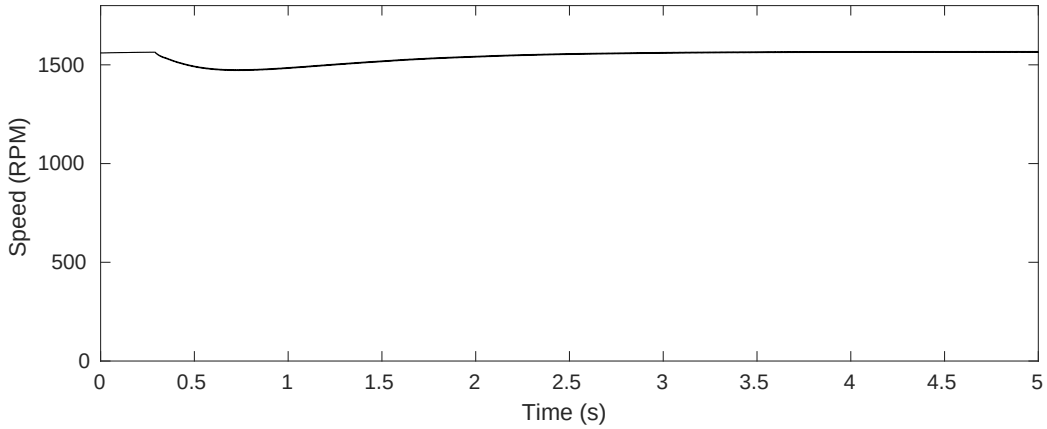

Figure 4.1: Speed of the machine with an open circuit fault.

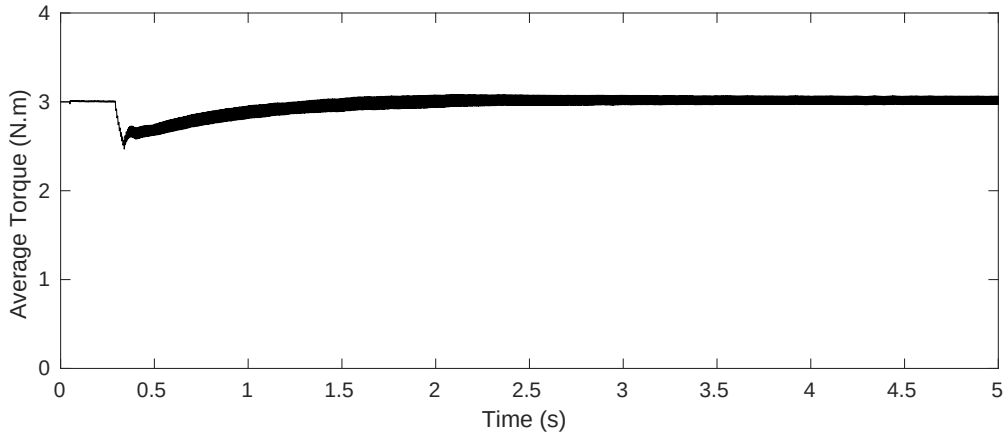

Figure 4.2: Average torque of the machine with an open circuit fault.

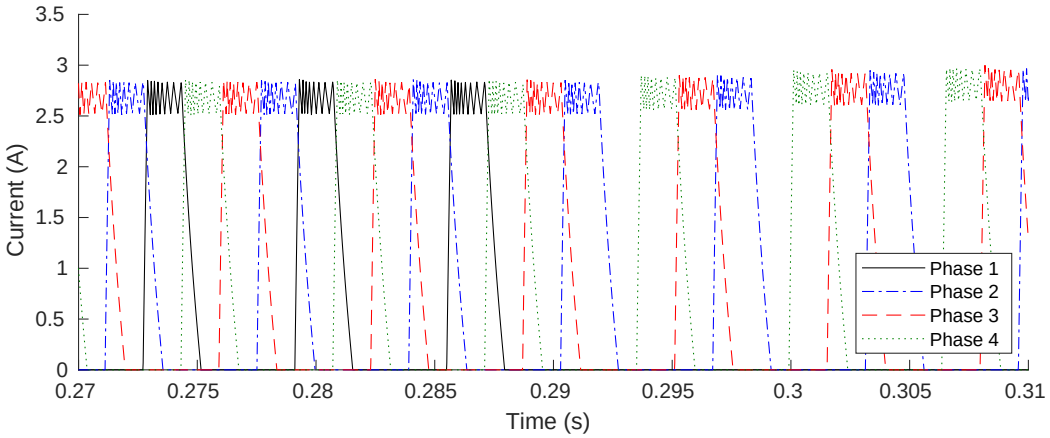

(a) Currents at the time of the fault.

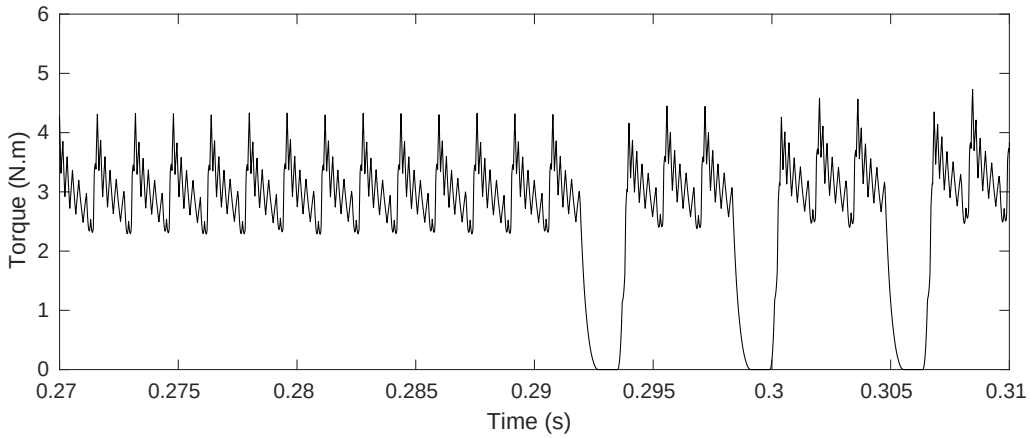

(b) Torque at the time of the fault.

Figure 4.3: Current and torque at the time of the open circuit fault.

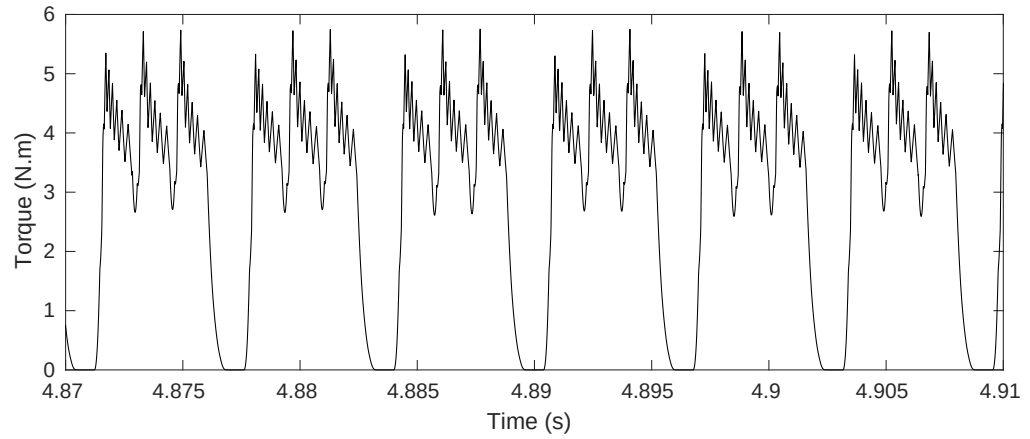

(a) Torque after the machine stabilized.

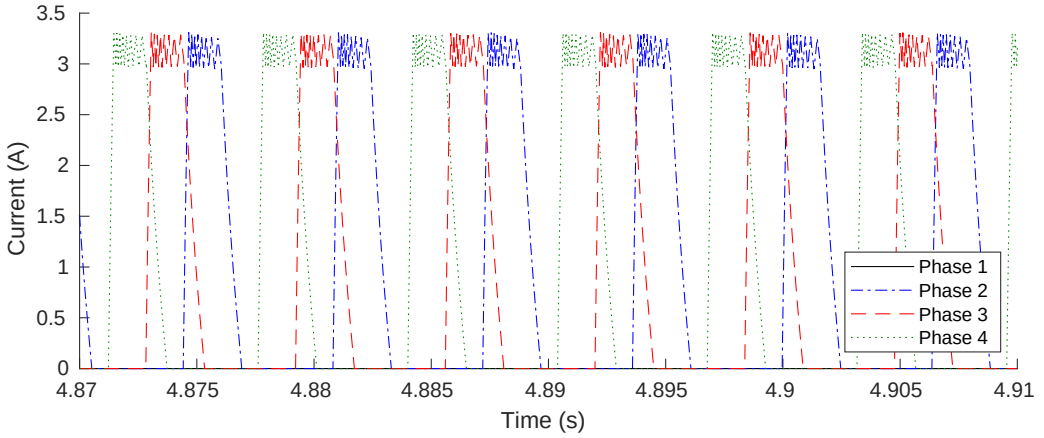

(b) Currents after the machine stabilized.

Figure 4.4: Current and torque after the machine stabilized from the open circuit fault.

this does not affect the machine at steady state to severely. However, it can be a problem at the start since if the rotor is at the position where the faulty phase should conduct it will not have the torque to move out of this position.

In table 4.1 the numerical results of the machine are represented. It can be seen that the ripple got considerably higher due to the fact that one torque pulse disappeared. However the electrical power got actually slightly lower, around 0.4 %.

Aspect	Value	Units
Torque Ripple	192.6	%
Average Electrical Power	509.5	W

Table 4.1: Results for an open circuit fault of the normal machine.

4.1.2 Short-circuit

In this subsection a short circuit in phase 1 of the machine will be presented and analyzed. As already mentioned in the previous chapter, this short-circuit will comprise of the one hundred and fifty most centered turns of the coil.

In figures 4.5 and 4.6 the speed and torque of the machine are presented respectively. It can be seen that the curves are similar with the ones from the open circuit case, where drops in the speed and average torque are observed but the machine being able to compensate them further in time.

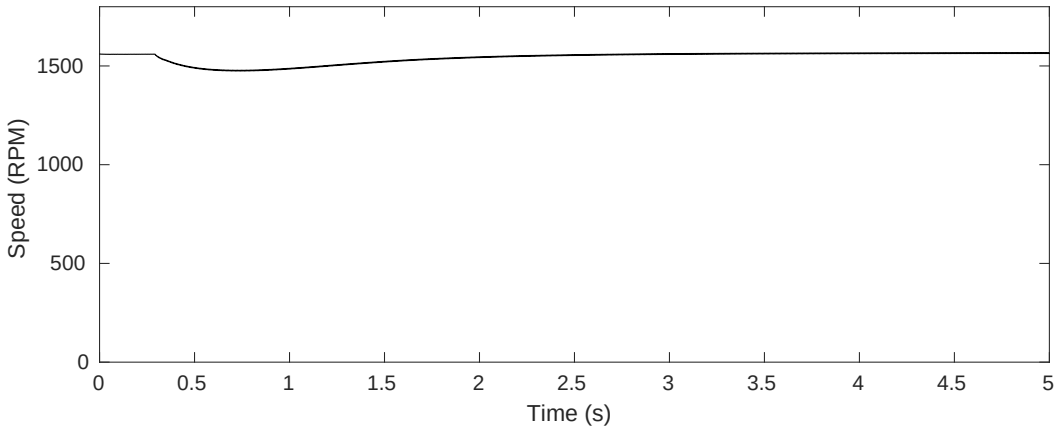

Figure 4.5: Speed of the machine with a short circuit fault.

In figures 4.7a and 4.7b the torque and currents measured are represented at the time of the fault. It can be seen that, despite of the current measured from the coil 1 does not suffer a great difference, the torque goes to near zero values.

This occurs because in the shorted turns a back emf will appear due to the variations of the flux in the healthy turns. This back emf will induce an opposite signed current

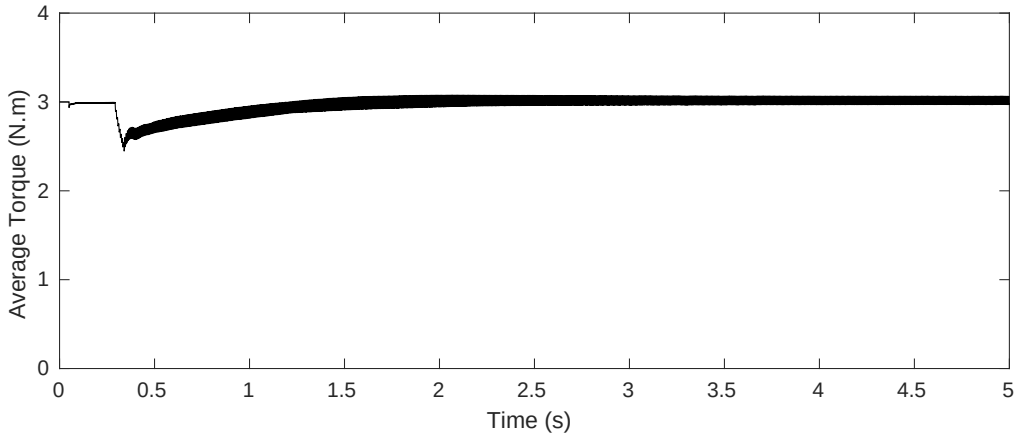

Figure 4.6: Average torque of the machine with a short circuit fault.

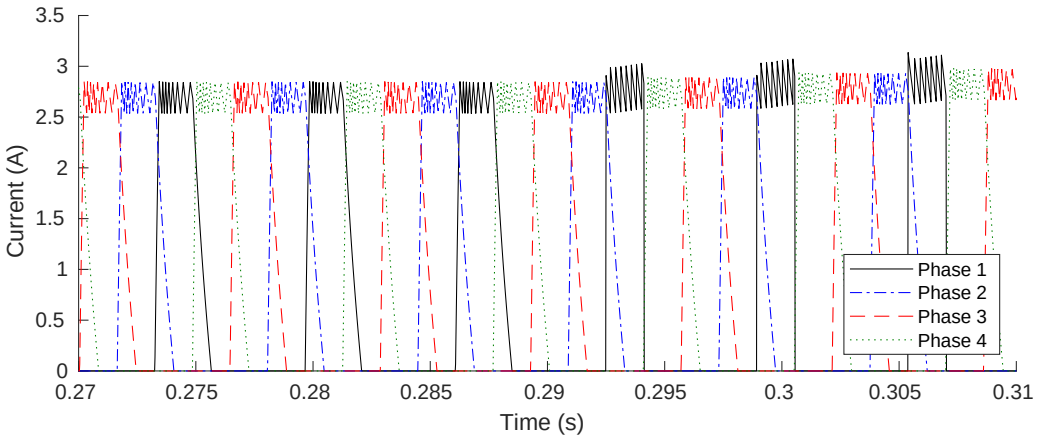

(a) Currents at the time of the fault

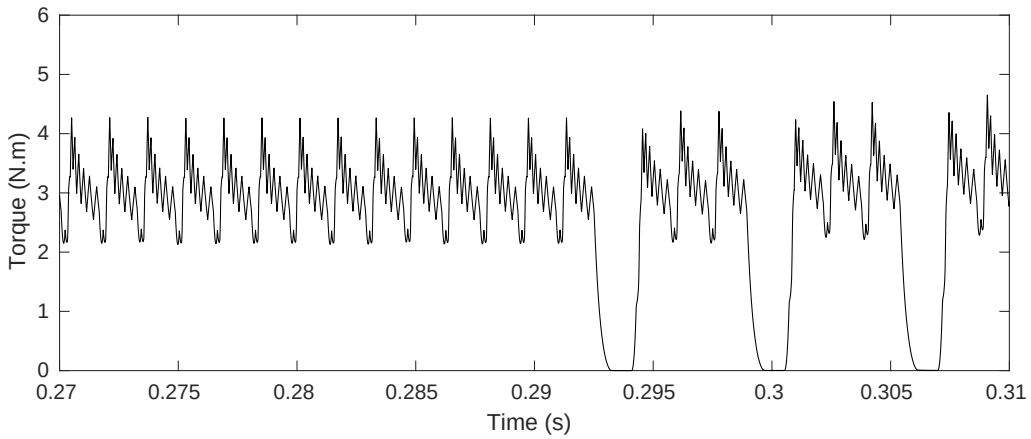

(b) Torque at the time of the fault

Figure 4.7: Torque and currents at the time of the short-circuit fault.

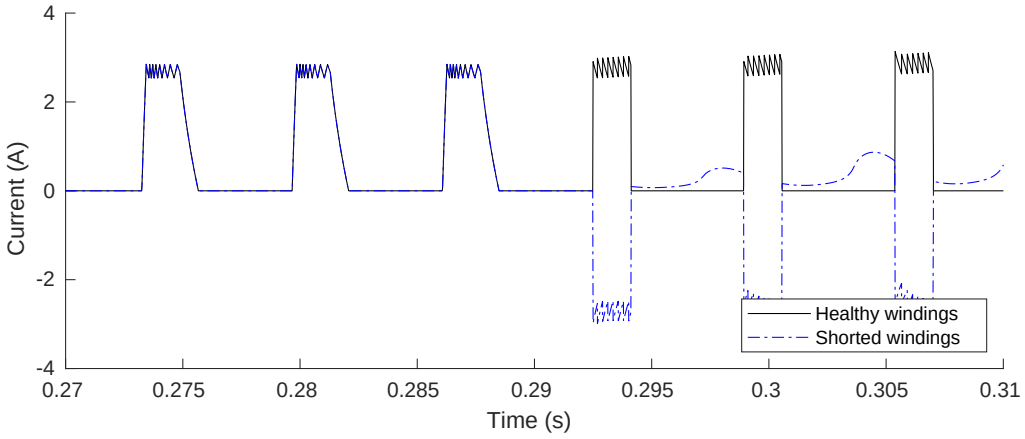

Figure 4.8: Normal current and shorted current of phase 1.

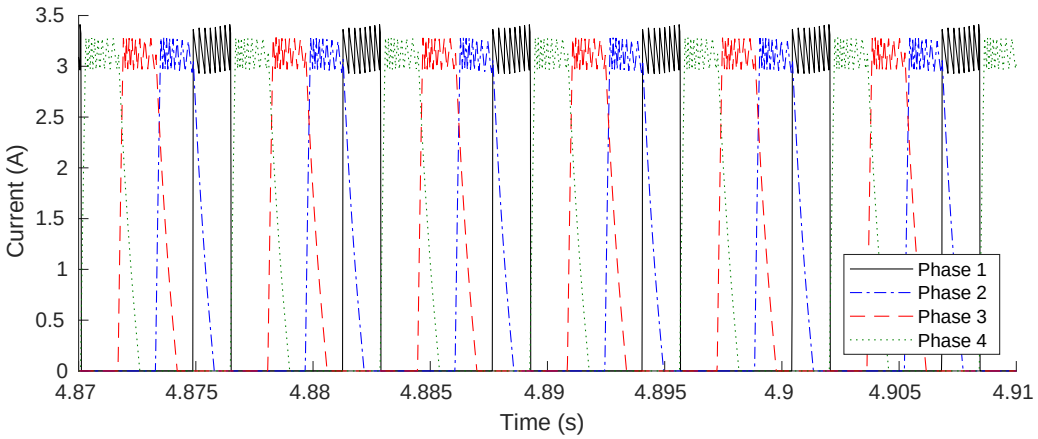

(a) Currents after the machine stabilized.

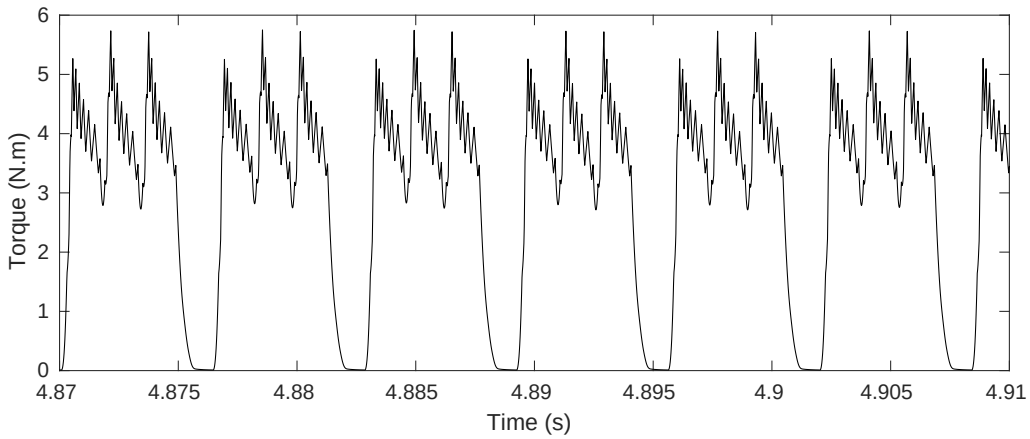

(b) Torque after the machine stabilized.

Figure 4.9: Torque and currents after the machine stabilized from the short-circuit fault.

in the shorted turns that will resist flux change. The healthy and short turns current are represented in figure 4.8. Due to the currents having opposite signs, the flux in the machine will be smaller and by that diminishing the torque supplied by the faulty phase.

Due to having less torque available the machine will make a compensation, like in the open circuit fault case, where the PI controller will rise the reference current for the hysteresis controller in order to rise the mean torque. This compensation in current and torque can be observed in figures 4.9a and 4.9b.

In table 4.2 the numerical results of the machine can be observed. As with the open circuit fault case, it can be noticed that the ripple increased dramatically. It can be seen that the electrical power in this case has risen slightly.

Aspect	Value	Units
Average Electrical Power	512.1	W
Torque Ripple	191.7	%

Table 4.2: Results for a short circuit fault of the normal machine.

4.2 Proposed Solution

The proposed alteration to the machine studied in Chapter 3 consists in a tweak in its coils and a semi new current control method. The coil tweak is basically dividing the coil in two halves with the same number of turns. This construction proposal is shown in figure 4.10.

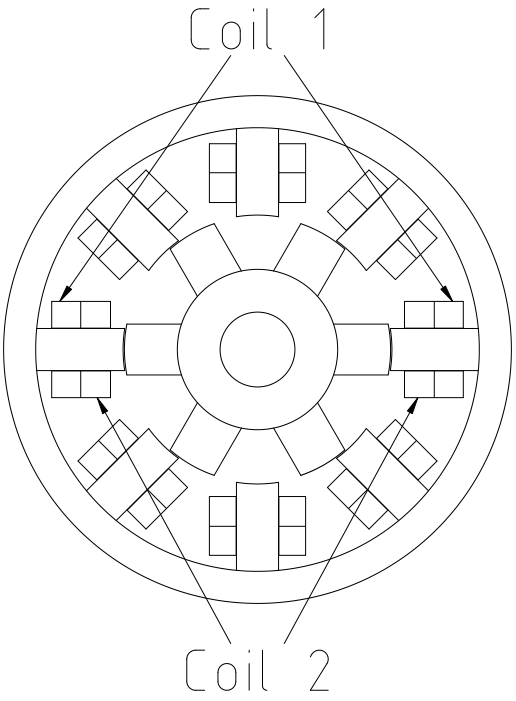

Figure 4.10: Schematic representation of the proposed coil solution.

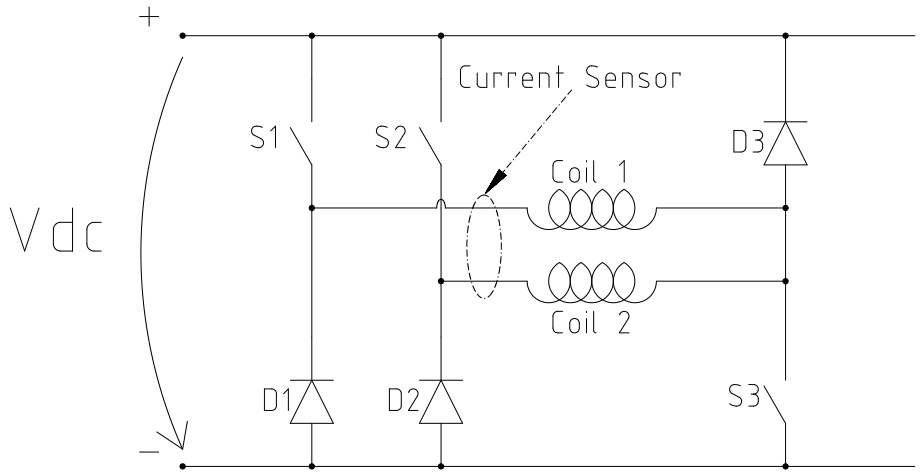

Figure 4.11: Converter for the machine solution.

It should be mentioned that this coil arrangement idea was already proposed by Miller in [13], however in the presented article no study was made and it was only mentioned what results could be expected from it.

Were, nonetheless, found similar solutions. In [31] it is described a situation, for a double channel machine, in which each pole is a coil controlled separately.

About the converter, a change had to be made for it to work with this arrangement of the coils. If the converter used was the normal asymmetric bridge with the two coils in parallel, the coils would make a close path and conduct to each other instead of the diodes.

The converter used is represented in figure 4.11. However, if it was used a full converter for each half coil of the machine it would also work.

4.2.1 *simulink*® implementation

For the implementation of this solution changes had to be made to the *simulink*® model. No changes were need in *Flux2D*® since in chapter 3 were already obtained the flux characteristics in function of both coils current $\Psi_i(i_1, i_2, \theta)$.

4.2.1.1 Coil and converter

However the *simulink*® changes made were only to the coil and converter. In figure 4.12 it is represented the inside of a phase block. It can be seen that it its very similar with the one from the normal machine with a bit more complexity.

In figure 4.13 it is shown the implementation the coil block in the proposed solution machine. Inside it there are two blocks with the implementation of each coil.

Inside *coil1* and *coil2* blocks it is implemented the equivalent circuit for each coil. They are represented in figures 4.14a and 4.14b, respectively. Both diagrams are very similar, however they differ in the look up table implementation. Another aspect that should be mentioned is the switches in series and parallel with the coils, they serve to provoke open

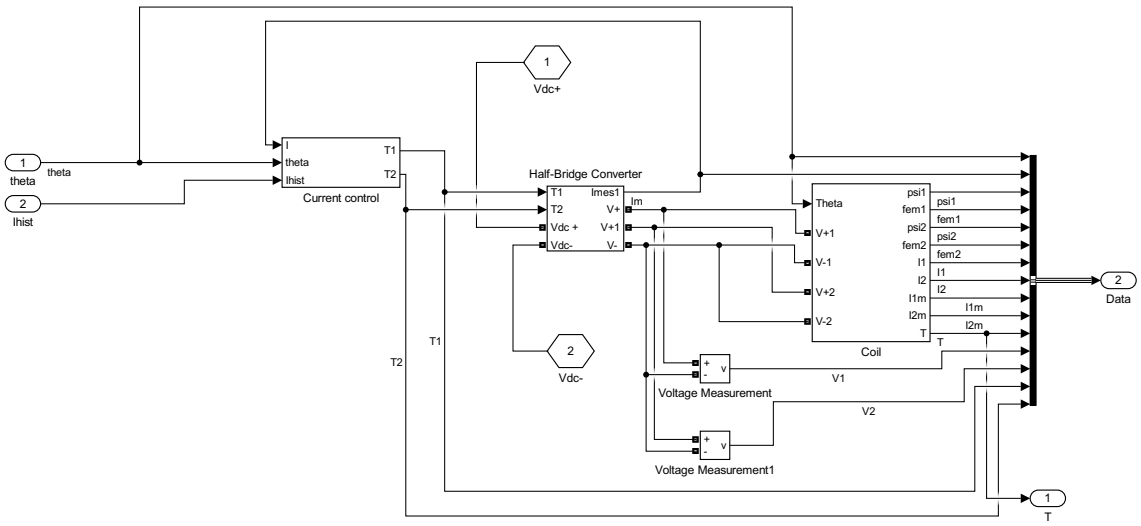

Figure 4.12: *Simulink*® implementation of a phase.

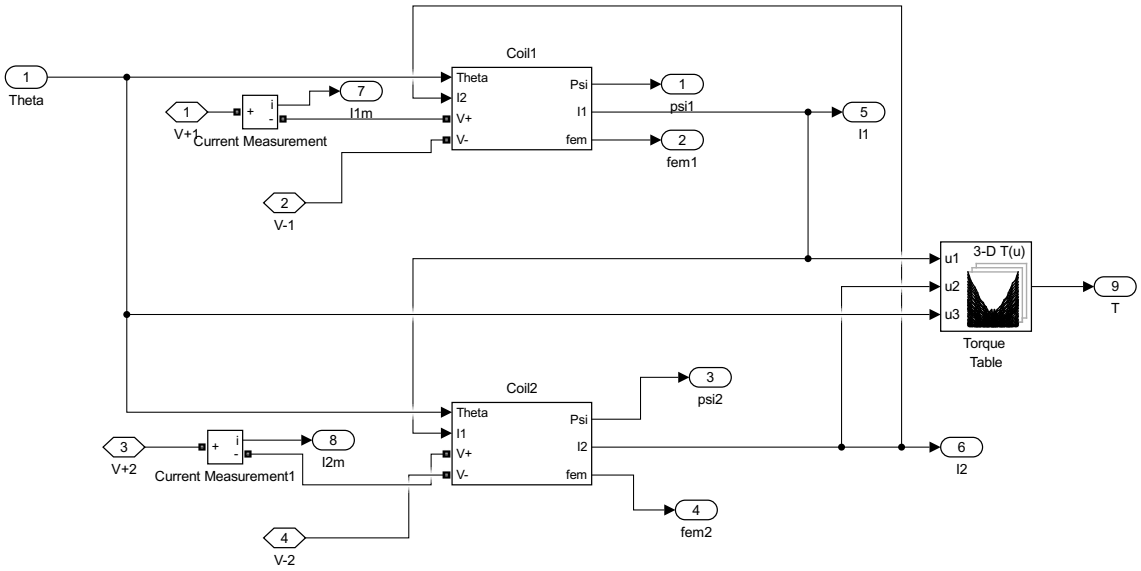

Figure 4.13: The *coil* block implementation.

circuit and short-circuit faults respectively. The switches signals are independent of each other.

It should also be noticed that the coils resistance is divided in two. This is to in the case of a short circuit the voltage source does not get directly shorted to the neutral or the simulation would throw an error. The resistance on the right side of the switched is 1.17 Ω and the one on the left is 0.13 Ω.

Regarding the converter, its implementation is represented in figure 4.15. It can be seen that its implementation is concordant with the diagram presented in 4.11.

It should also be mentioned that the voltage supply was changed to 400 V.

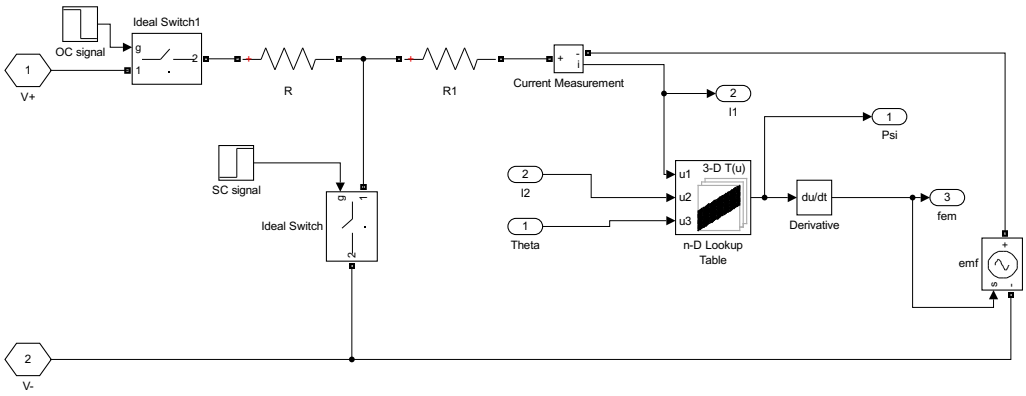

(a) *Simulink*® implementation of coil 1 of phase 1

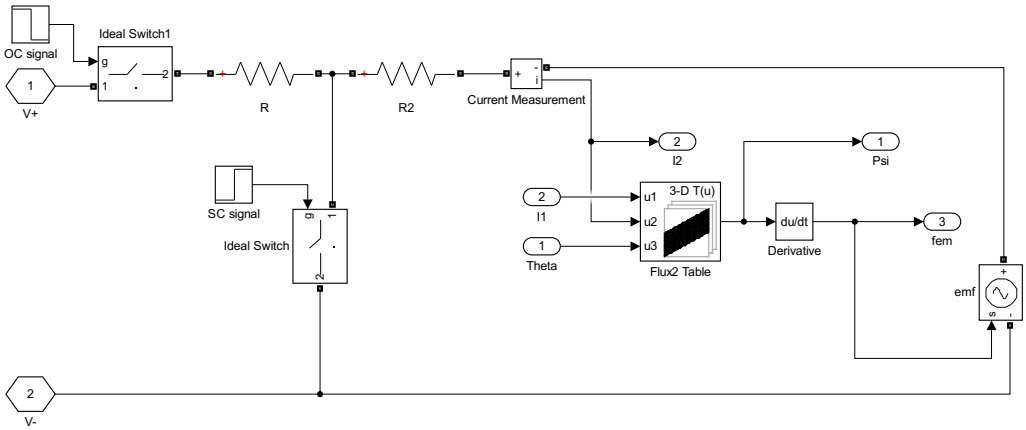

(b) *Simulink*® implementation of coil 2 of phase 1

Figure 4.14: The *coil1* and *coil2* blocks.

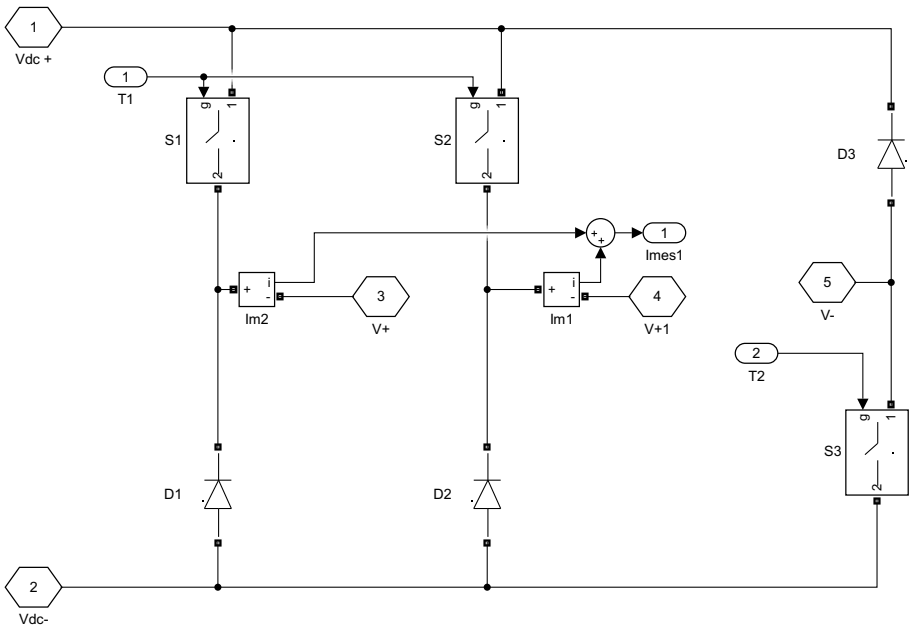

Figure 4.15: Implementation of the converter for the proposed solution.

4.2.1.2 Control

The motor with this strategy continues to be controlled by the same PI controller, with the average torque as the control variable and a reference current as the output signal.

However, having now two coils to control, changes were needed. The CHC now controls the sum of the two currents, as in figure 4.15 shows that the sum of the two currents is now the output measure from the sensor. For this reason the hysteresis band was changed to 600 mA. As it will be seen forward, this small change will allow that as soon as an open circuit fault occurs in one coil, the other one will be able to compensate it immediately.

4.2.2 Starting simulation

For demonstration purposes, it was also performed a simulation of the proposed solution motor starting until it reached steady state, for a reference torque of 3 N.m. The speed and average torque during start are represented in figures 4.16 and 4.17, respectively. It can be noticed that the curves obtained with this solution are similar to the ones obtained for the normal machine, indicating that in normal conditions the mechanical operation should not be too much affected. However, a more detailed analysis will be done in the steady state case.

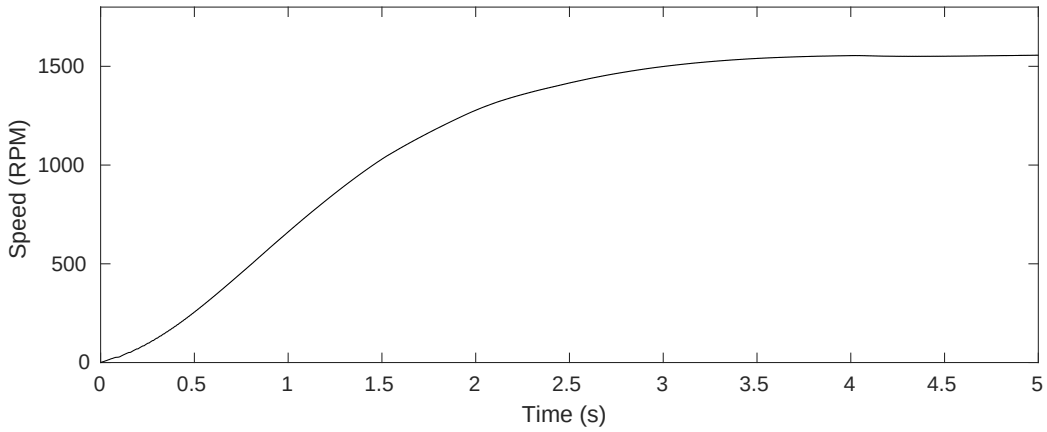

Figure 4.16: Speed of the solution machine during start.

4.2.3 Steady State

As it was done with the normal machine, a steady state was simulated for the proposed solution. The speed and average torque are represented in figures 4.18 and 4.19. As in the case of the start, not much difference is observed in this curves.

In figure 4.20 the total torque is presented for a shorter interval of time. As with the normal machine, the middle of the interval is the time at which faults will occur in the fault simulations. This image will also serve for comparison with the faulty cases.

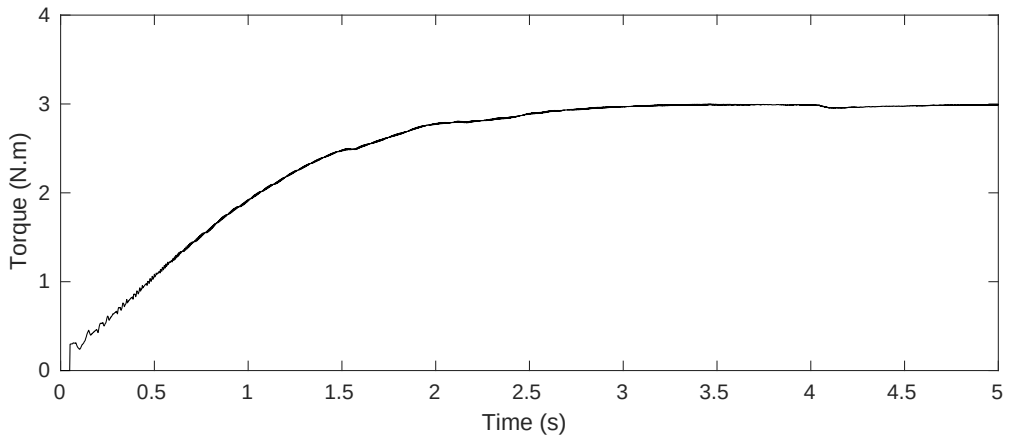

Figure 4.17: Average torque of the solution machine during start.

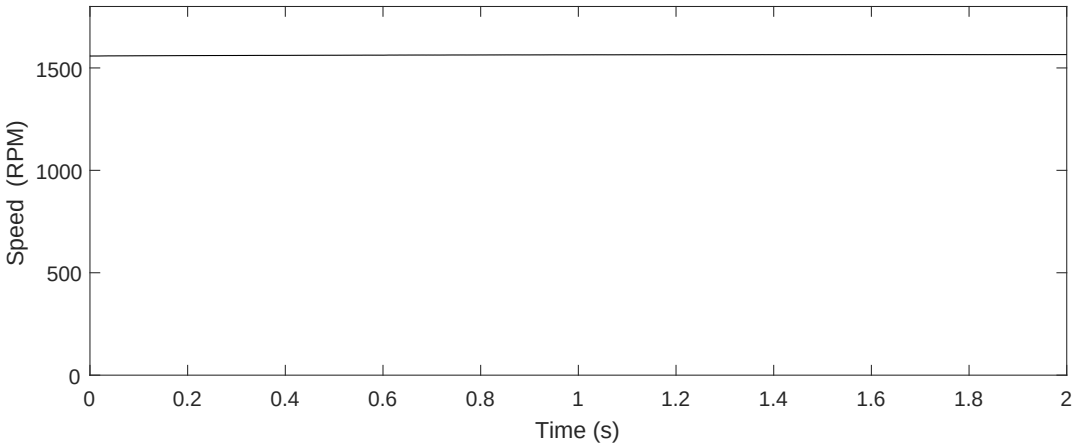

Figure 4.18: Speed of the solution machine in steady state.

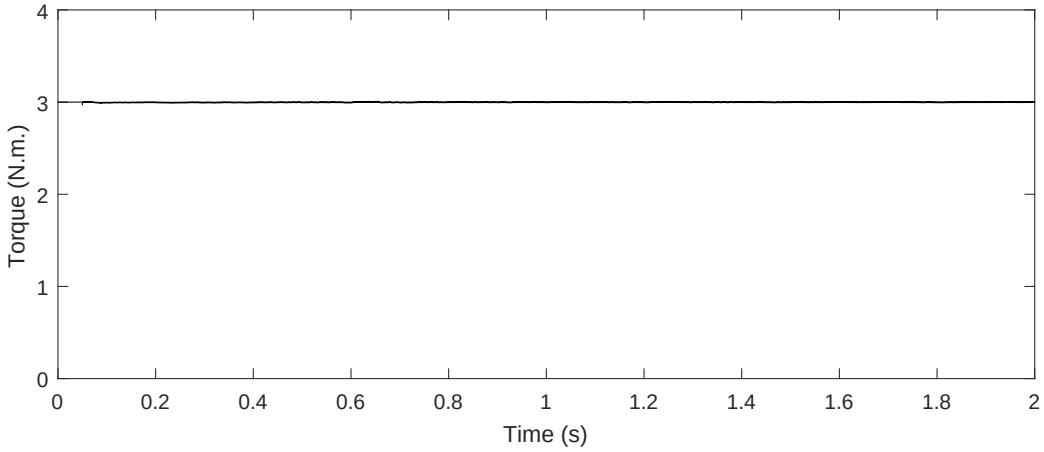

Figure 4.19: Average torque of the solution machine in steady state.

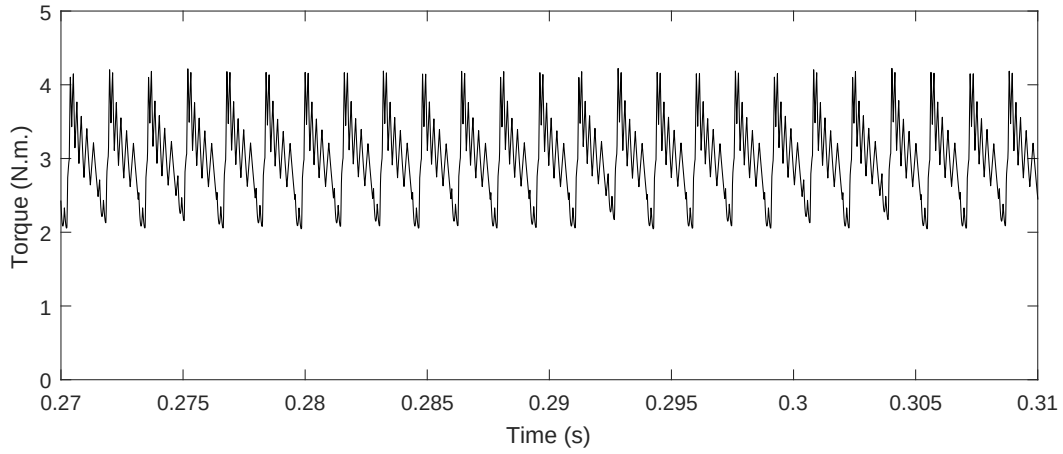

Figure 4.20: Torque of the solution machine in steady state.

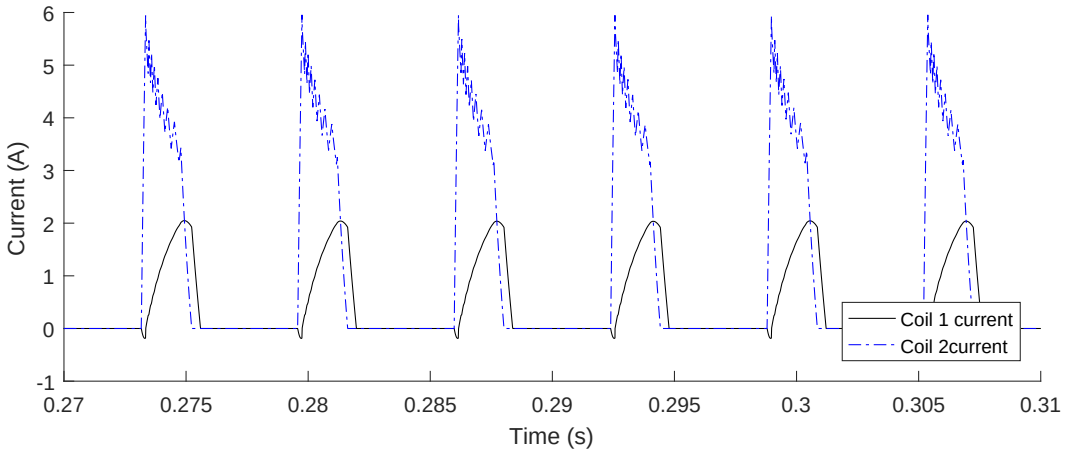

Figure 4.21: Measured and coils 1 and 2 currents of phase 1 in steady state.

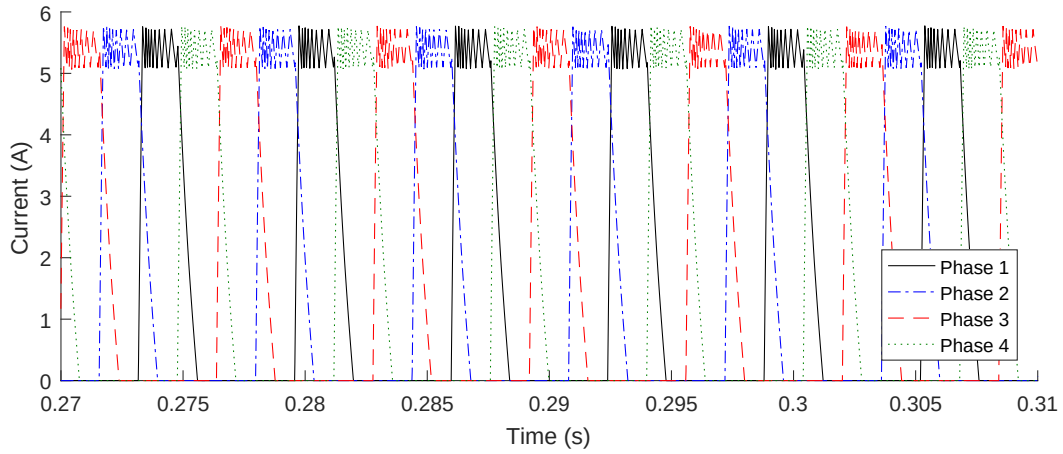

Figure 4.22: Measured currents from all phases in steady state.

In figure 4.21 the currents for both coils of phase 1 are represented. In figure 4.22 it is represented the control current measured for all phases. Comparing its the value with the one from normal machine it can be seen the value is about the double, as should be expected. It should be mentioned that the sum of both currents in figure 4.21 is equal to the total measured current of phase 1 represented in figure 4.22. This is part of the mechanism behind the fault tolerance of the method.

It should also be noticed that the currents from figure 4.21 present differences in amplitude and form despite the coils having the same number of turns. This can be explained by the flux characteristics of both coils not being exactly equal, as already stated in chapter 3. This difference will allow a coil to dominate the dynamics of the system.

In table 4.3 the numerical results of this steady state are presented. It can be seen a that this method consumes around 1.6% more electrical power and has a ripple 6% higher compared with the normal machine in non fault conditions. However in the next chapter it will be shown the advantages of this construction.

Aspect	Value	Units
Average Electrical Power	519.8	W
Torque Ripple	74.2	%

Table 4.3: Numerical results for the steady state of the proposed solution machine.

Chapter 5

Results from the solution motor faulty cases

In this section the results from the motor with solution will be shown and analyzed. The results from fault cases will be shown and discussed by comparing them with the normal motor fault cases. The cases studied: an open circuit in coil 1, an open circuit in coil 2, a short-circuit in coil 1. All cases will start with the machine in steady state with an average torque of 3 N.m and an average speed of 1565 RPM.

5.1 Coil 1 of phase 1 in open circuit

During the simulation, at time $t = 0.29$ s, an open circuit fault was introduced to the coil 1 of phase 1. The speed and average torque are represented in figures 5.1 and 5.2. In figure 5.3 the total torque at the time of the fault is represented. Comparing the previous figures with the equivalent from the steady state 4.18, 4.19 and 4.20, it can be seen that this type of fault does not affect significantly the mechanical output of the machine.

In figure 5.4 currents of coil 1 and coil 2 are represented at the time of the fault. It can be seen that when coil 1 gets faulty it stops conducting and the loss of its current will be compensated by coil 2.

The fastness of the compensation is possible because the reference current will force a current with its value on the healthy coil 2. In figure 5.5 this effect can be visualized. In the next current pulse after the fault occurrence the current from coil 2 is equal to the total current controlled.

The analytic results for the machine are presented in table 5.1. It can be seen that the electric power increases around 0.6%, however the torque ripple maintained its value instead of increasing significantly as in the case with the normal machine. This can be seen as a good improvement from the open circuit case in the normal machine.

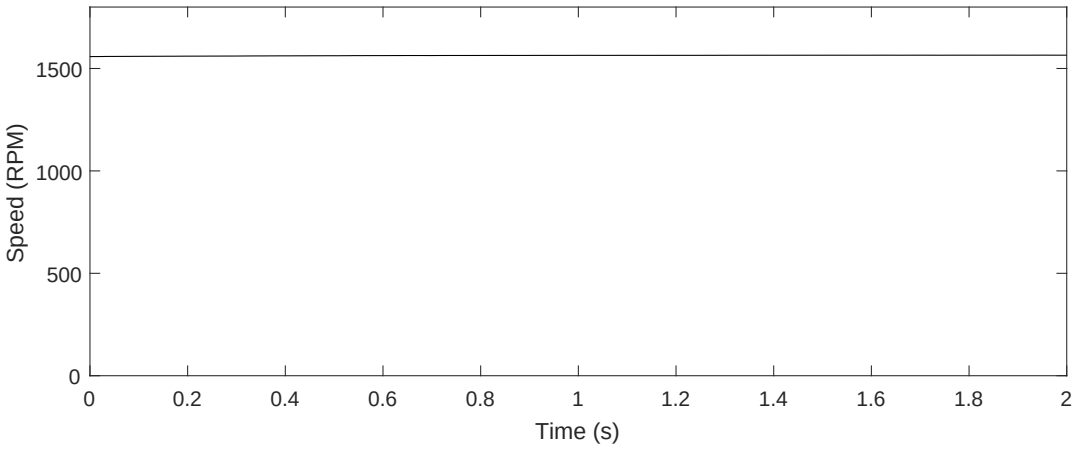

Figure 5.1: Speed with an open circuit fault on coil 1.

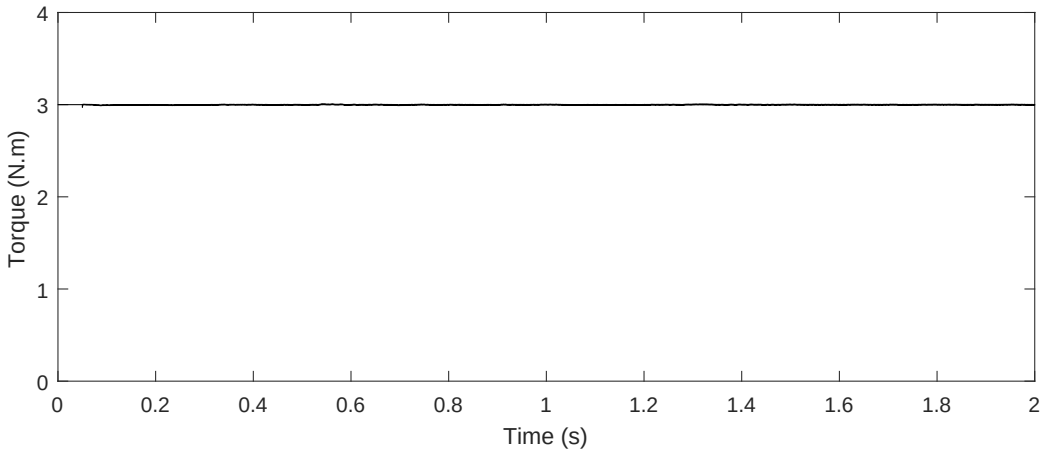

Figure 5.2: Average torque with an open circuit fault on coil 1.

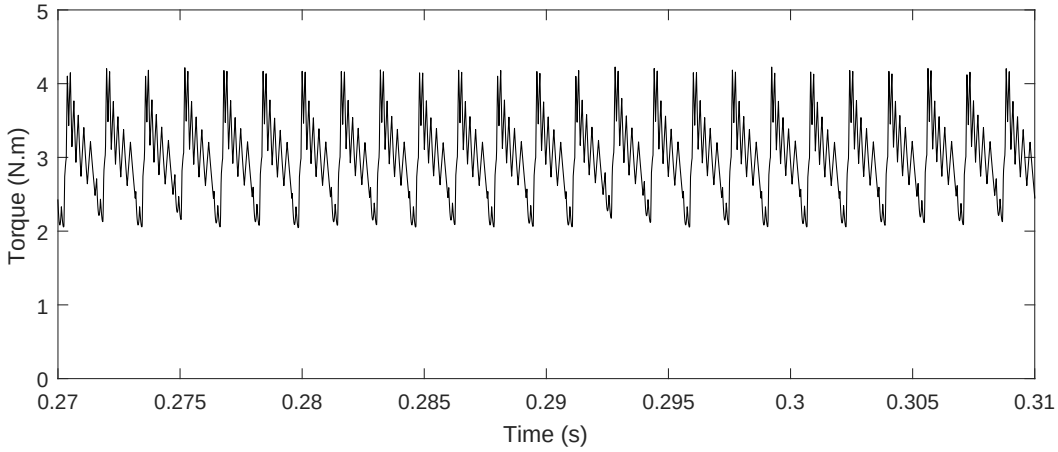

Figure 5.3: Torque with an open circuit fault on coil 1.

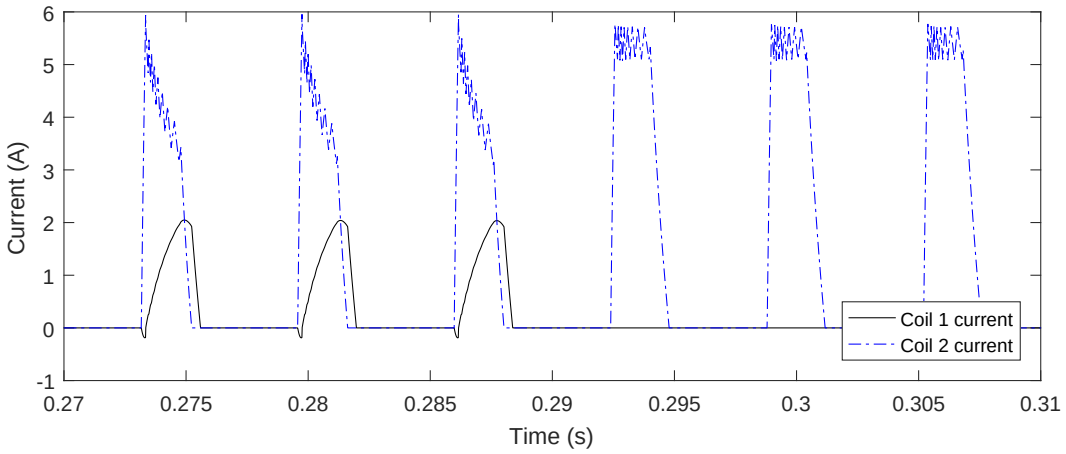

Figure 5.4: Currents of both coils of phase 1 with an open circuit fault on coil 1.

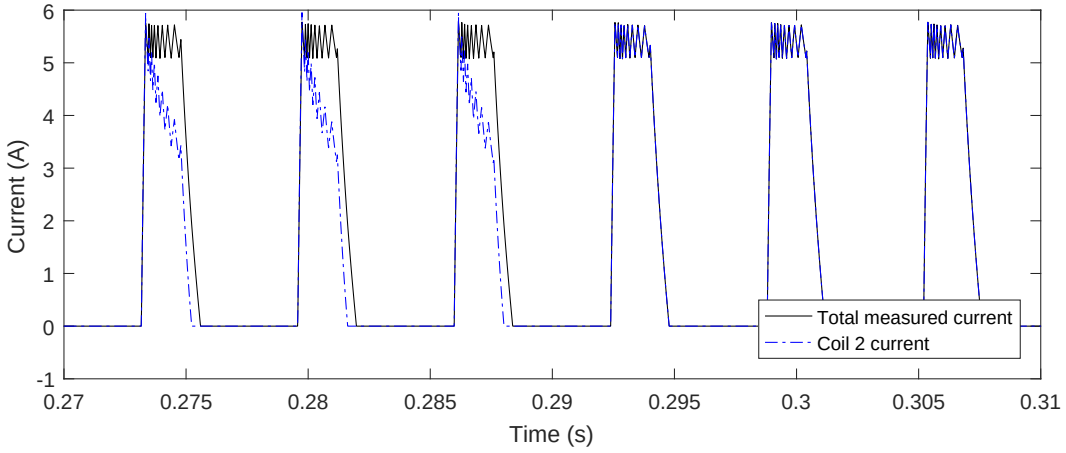

Figure 5.5: Measured and coil 2 currents of phase 1 with an open circuit fault on coil 1.

Aspect	Value	Units
Torque Ripple	74.2	%
Average Electrical Power	522.8	W

Table 5.1: Results for the proposed solution machine with an open circuit fault in coil 1.

5.2 Coil 2 of phase 1 in open circuit

During the simulation, at time $t = 0.29$ s an open circuit fault was introduced to the coil 1 of phase 2. In figures 5.6 and 5.7 the rotor speed and average torque can be observed. In figure 5.8 it is represented the total torque in a narrower time interval around the time of the fault. In can be seen, similarly to a open circuit fault in coil 1, that the mechanical output of the machine is almost unaffected.

In figure 5.9 currents from both coils of phase 1 are represented. It can be seen that at the time of the fault coil 2 stops conducting and a compensation in coil 1 will occur,

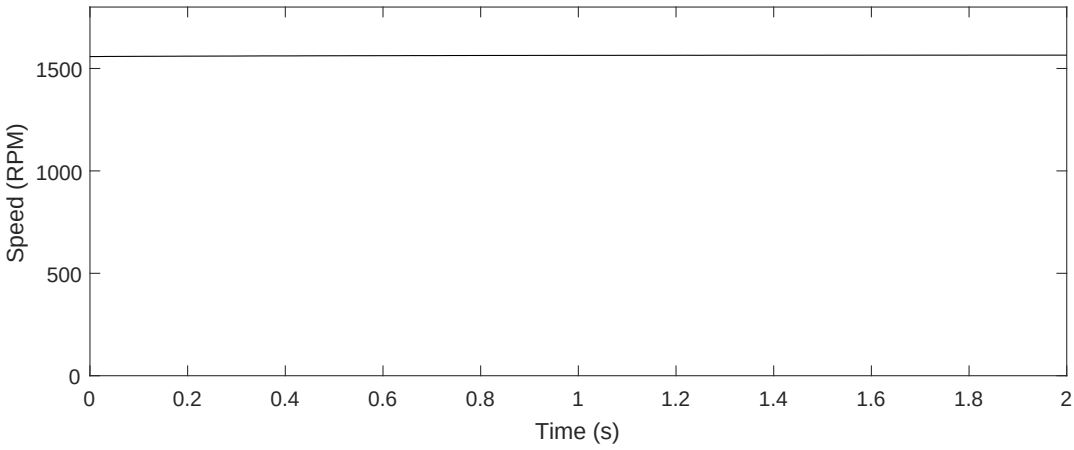

Figure 5.6: Speed with an open circuit fault on coil 2.

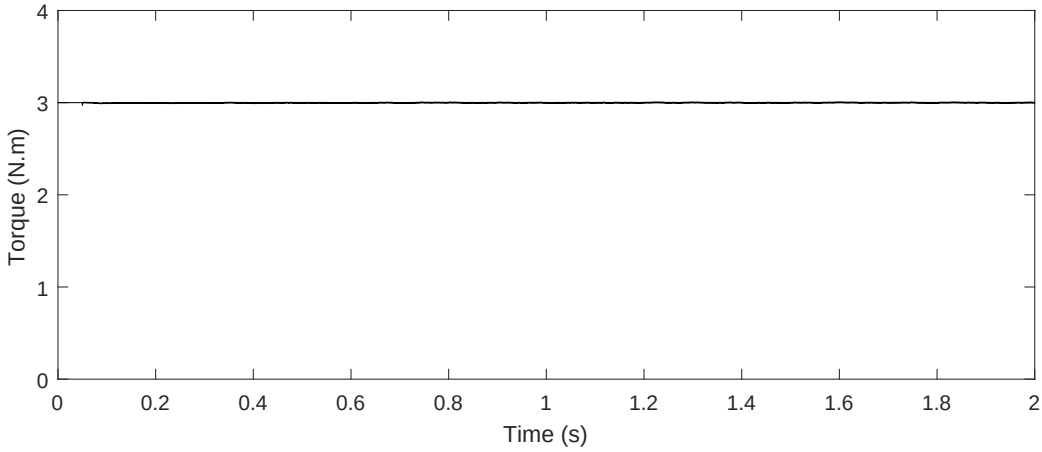

Figure 5.7: Average torque with an open circuit fault on coil 2.

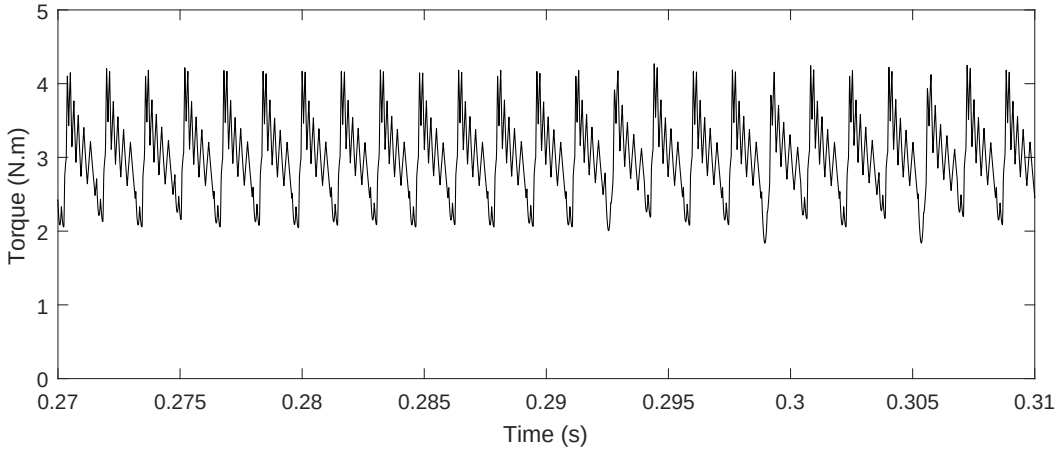

Figure 5.8: Torque with an open circuit fault on coil 2

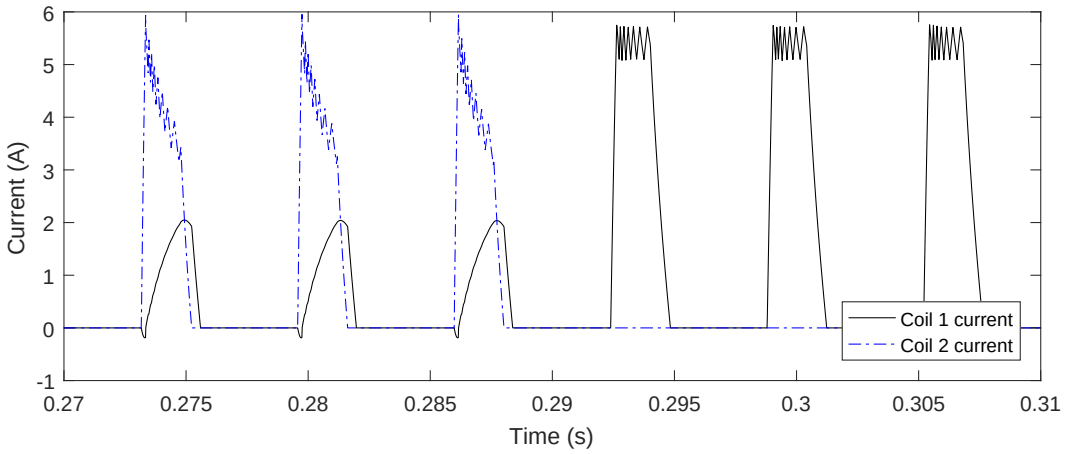

Figure 5.9: Currents of both coils of phase 1 with an open circuit fault in coil 2.

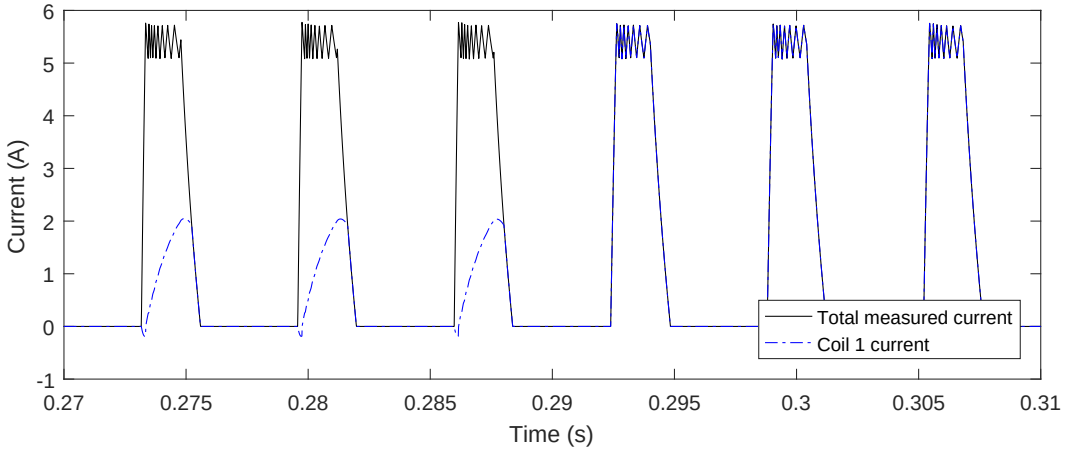

Figure 5.10: Measured and coil 1 currents of phase 1 with an open circuit fault on coil 1.

similar to the previous case.

This compensation is possible because of the same mechanism described in the previous fault since it's the same type of fault.

The numerical results for the machine are presented in table 5.2. In this case the ripple actually increased however still much less than the normal machine open circuit. The electrical power as risen the same as the previous case. With this two cases having good results it can be said that the method is effective for open circuit faults in windings.

Aspect	Value	Units
Torque Ripple	84.6	%
Average Electrical Power	522.8	W

Table 5.2: Results for the proposed solution machine with an open circuit fault in coil 2.

5.3 Coil 1 of phase 1 in short circuit

During the simulation, at time $t = 0.29$ s a short circuit fault was introduced to the coil 1 of phase 1. In figures 5.11 and 5.12 the rotor speed and average torque can be observed. It can be seen, like in the case of the normal machine with a short circuit, that the speed and average torque will have a drop at the time of the fault but will again rise to their normal values.

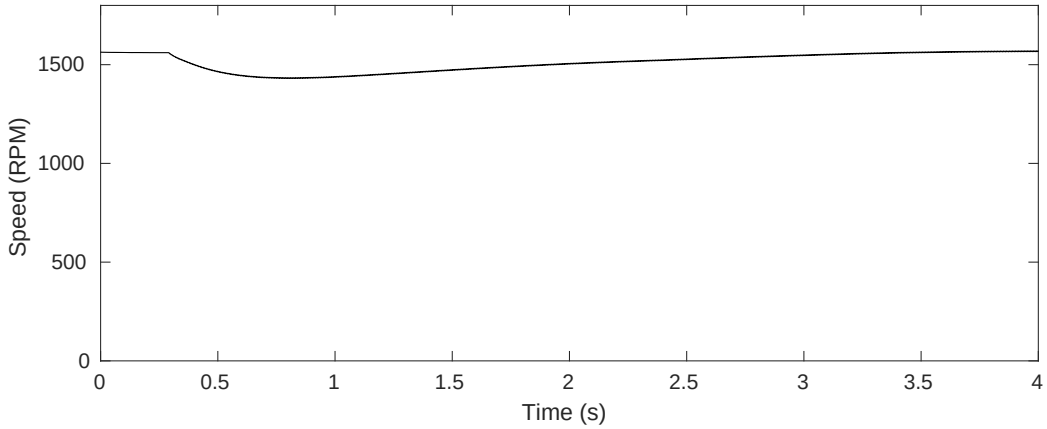

Figure 5.11: Speed with a short circuit fault on coil 1.

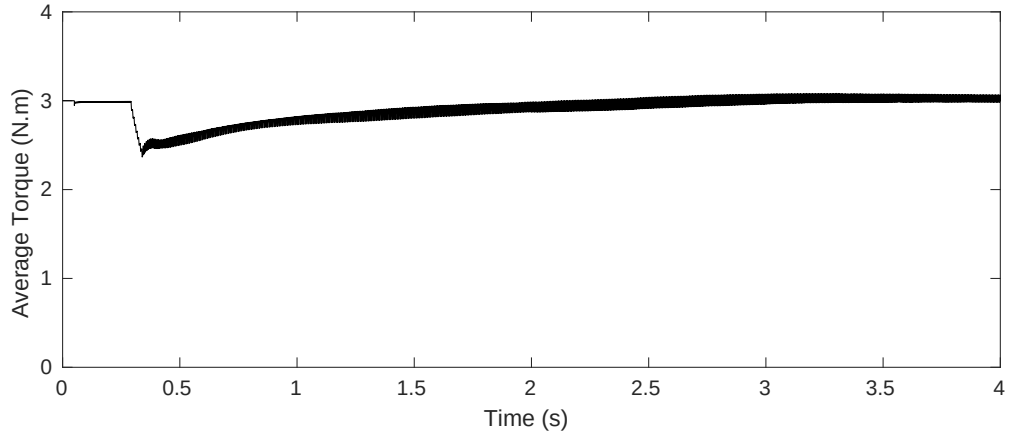

Figure 5.12: Average torque with a short circuit fault on coil 1.

In figures 5.13a and 5.13b the torque and total measured currents are represented at the moment of the fault. It can be seen that the current maintains but the torque goes to near zero values, like in the normal machine short circuit case.

This is because, like in the shorted case of the normal machine, a back emf will be induced in coil 2, since the coil is completely shorted, and a current with the opposite signal will appear in coil 2, this is represented in figure 5.14. This will reduce the flux and by that reduce the torque supplied from the phase.

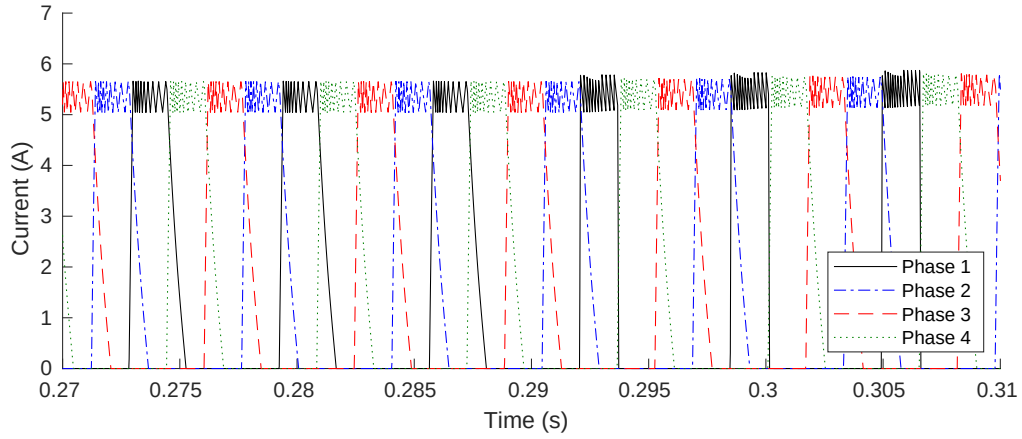

(a) Measured total currents at the time of the fault.

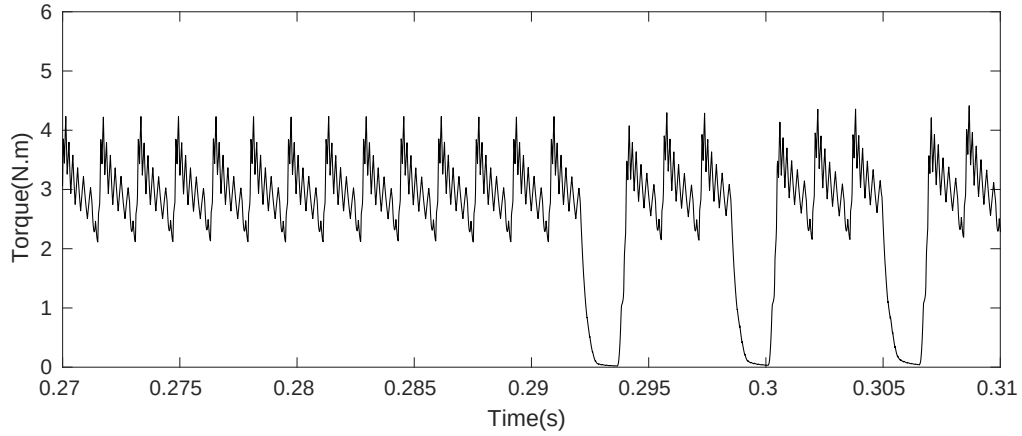

(b) Torque at the time of the fault.

Figure 5.13: Currents and torque at the time of the short circuit fault on coil 1.

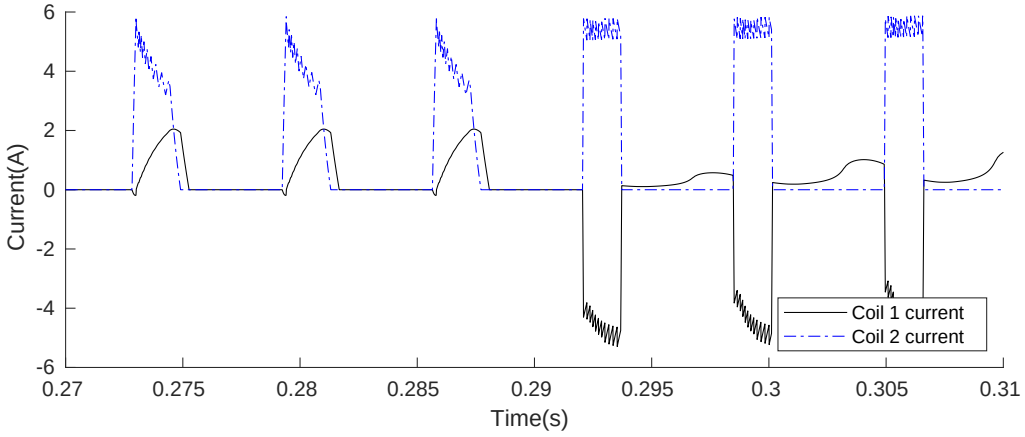

Figure 5.14: Coil 1 and coil 2 currents of phase 1 during a short circuit fault.

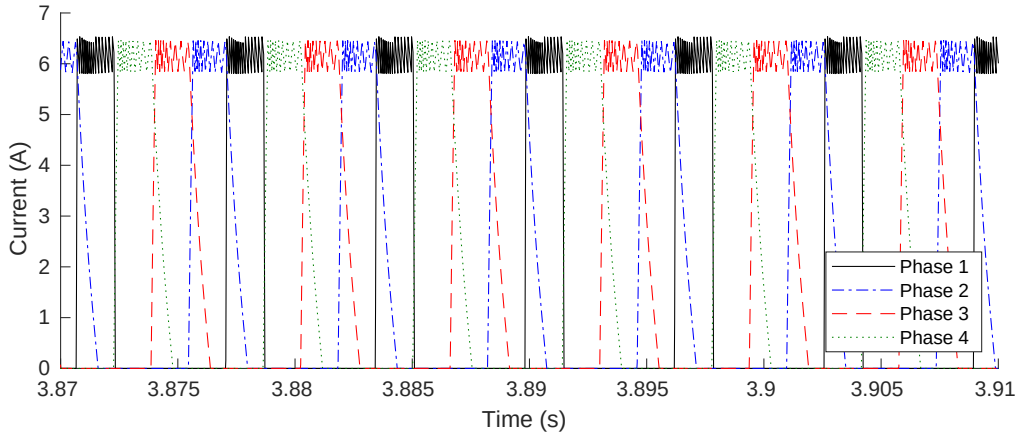

(a) Measured total currents after the machine stabilized.

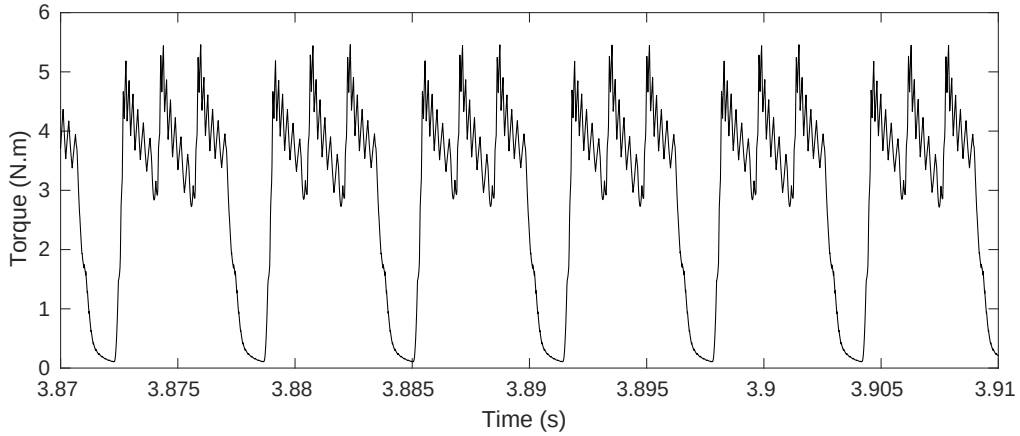

(b) Torque after the machine stabilized.

Figure 5.15: Currents and torque after the machine stabilized from the short circuit fault.

However, just like in normal machine faulty cases, a compensation by the other phases will occur further in time by the mechanisms already discussed in the normal machine. This can be seen in figures 5.15a and 5.15b.

In table 5.3 the numerical results can be seen for the short-circuit in coil 1. It can be seen that the electrical power rises even more that the open circuit cases (2.6%). The ripple also greatly increases comparing to the non faulty and open circuit cases, however it still got lesser than the short circuit case in the normal machine.

Aspect	Value	Units
Torque Ripple	178.8	%
Average Electrical Power	533.2	W

Table 5.3: Results for the proposed solution machine with a short circuit fault in coil 1.

Chapter 6

Conclusions and future works

6.1 Final conclusions

In this dissertation it was presented a new passive method, consisting in some tweaks in the coils, converter and control, for dealing with open circuit faults in windings. It were performed finite element analysis to obtain the magnetic and torque characteristics using the software *Flux2D*®. This was followed by dynamic simulations in the software *simulink*® to compare a normal machine with a machine with the proposed solution, both with normal functioning and under fault conditions.

It was seen that the machine with the solution, although with a slight worse performance with no faults, performed better in open circuit faults comparatively to the normal machine. Short circuit faults were also presented however without achieving the good results that the open circuit cases offered.

It also should be noticed that the short-circuit cases were very specific as one should take into account that the performance of the machine under short-circuit will greatly depend on the number of shorted turns.

The results of this dissertation gave origin to a paper entitled "A novel spilt-winding fault-tolerant approach for a Switched Reluctance Motor" on the same subject. This paper was presented in IEEE/IES IECON conference in October 2019.

6.2 Future works

To complete the work started by this dissertation some future work is required. The most imperative being the construction of a physical prototype of the machine to confirm experimentally if the method has the results it shown in simulation.

Another important work that should be performed is the analysis of the machine with

the proposed method with different short circuit cases with less shorted turns. Associated with this should be done an investigation to modify the method to try to accommodate the short-circuit faults.

Finally, another study could be conducted in order to try to adapt the method to different and more complex control schemes such as neural networks or fuzzy logic.

Bibliography

[1] W. Ding, Y. Hu, L. Wu, and Y. Liu. "Fault-tolerant performance of a mutually coupled dual-channel switched reluctance generator under open-circuit faults." In: *2014 17th International Conference on Electrical Machines and Systems (ICEMS)*. 2014, pp. 1802–1807. DOI: 10.1109/ICEMS.2014.7013791.

[2] G. Han, H. Chen, and X. Shi. "Modelling, diagnosis, and tolerant control of phase-to-phase fault in switched reluctance machine." In: *IET Electric Power Applications* 11.9 (2017), pp. 1527–1537. ISSN: 1751-8660. DOI: 10.1049/iet-epa.2017.0185.

[3] L. Szabó, M. Ruba, C. Szász, V. Chindriş, and G. Husi. "Fault tolerant bio-inspired system controlled modular switched reluctance machine." In: *automatika* 55.1 (2014), pp. 53–63.

[4] I. Husain, A. Radun, and J. Nairus. "Fault analysis and excitation requirements for switched reluctance-generators." In: *IEEE Transactions on Energy Conversion* 17.1 (2002), pp. 67–72. ISSN: 0885-8969. DOI: 10.1109/60.986439.

[5] H. Chen, W. Yan, Q. Wang, S. Lu, and Z. Chen. "Modeling of a switched reluctance motor under stator winding fault condition." In: *2015 IEEE International Magnetics Conference (INTERMAG)*. 2015, pp. 1–1. DOI: 10.1109/INTMAG.2015.7157245.

[6] A. E. Fitzgerald, C. Kingsley, and S. Umans. "Electric Machinery." In: sixth edition. McGraw-Hill, 2003. Chap. 8.

[7] T. J. E. Miller. *Brushless Permanent-Magnet and Reluctance Motor Drives*. Oxford University Press, 1989. Chap. 7.

[8] A. Radun. "Generating with the switched reluctance motor." In: *Proceedings of 1994 IEEE Applied Power Electronics Conference and Exposition - ASPEC'94*. 1994, 41–47 vol.1. DOI: 10.1109/APEC.1994.316421.

[9] D. A. Torrey. "Switched reluctance generators and their control." In: *IEEE Transactions on Industrial Electronics* 49.1 (2002), pp. 3–14. ISSN: 0278-0046. DOI: 10.1109/41.982243.

[10] M. Barnes and C. Pollock. "Power electronic converters for switched reluctance drives." In: *IEEE Transactions on Power Electronics* 13.6 (1998), pp. 1100–1111. ISSN: 0885-8993. DOI: 10.1109/63.728337.

[11] C. M. Stephens. "Fault detection and management system for fault tolerant switched reluctance motor drives." In: *Conference Record of the IEEE Industry Applications Society Annual Meeting*, 1989, 574–578 vol.1. DOI: 10.1109/IAS.1989.96707.

[12] S. Gopalakrishnan, A. M. Omekanda, and B. Lequesne. "Classification and remediation of electrical faults in the switched reluctance drive." In: *IEEE Transactions on Industry Applications* 42.2 (2006), pp. 479–486. ISSN: 0093-9994. DOI: 10.1109/TIA.2006.870044.

[13] T. J. E. Miller. "Faults and unbalance forces in the switched reluctance machine." In: *IEEE Transactions on Industry Applications* 31.2 (1995), pp. 319–328. ISSN: 0093-9994. DOI: 10.1109/28.370280.

[14] V. K. Sharma, S. S. Murthy, and B. Singh. "Analysis of switched reluctance motor drive under fault conditions." In: *Conference Record of 1998 IEEE Industry Applications Conference. Thirty-Third IAS Annual Meeting (Cat. No.98CH36242)*. Vol. 1. 1998, 553–562 vol.1. DOI: 10.1109/IAS.1998.732372.

[15] B. Lequesne, S. Gopalakrishnan, and A. M. Omekanda. "Winding short circuits in the switched reluctance drive." In: *IEEE Transactions on Industry Applications* 41.5 (2005), pp. 1178–1184. ISSN: 0093-9994. DOI: 10.1109/TIA.2005.855051.

[16] H. Torkaman and E. Afjei. "Comprehensive Detection of Eccentricity Fault in Switched Reluctance Machines Using High-Frequency Pulse Injection." In: *IEEE Transactions on Power Electronics* 28.3 (2013), pp. 1382–1390. ISSN: 0885-8993. DOI: 10.1109/TPEL.2012.2205947.

[17] B. Ilhem, B. Amar, L. Abdesselam, B. Mouhamed, R. Fares, and B. Bachir. "Modeling and detection of eccentricity fault in Switched Reluctance Motor." In: *2011 10th International Conference on Environment and Electrical Engineering*. 2011, pp. 1–5. DOI: 10.1109/EEEIC.2011.5874721.

[18] D. G. Dorrell, I. Chindurza, and C. Cossar. "Effects of rotor eccentricity on torque in switched reluctance Machines." In: *IEEE Transactions on Magnetics* 41.10 (2005), pp. 3961–3963. ISSN: 0018-9464. DOI: 10.1109/TMAG.2005.855178.

[19] C. P. Weiss, A. Hofmann, F. Qi, and R. W. D. Doncker. "Analysis and modelling of rotor eccentricity for switched reluctance machines." In: *7th IET International Conference on Power Electronics, Machines and Drives (PEMD 2014)*. 2014, pp. 1–6. DOI: 10.1049/cp.2014.0337.

[20] N. S. Gameiro and A. J. M. Cardoso. "Analysis of SRM drives behaviour under the occurrence of power converter faults." In: *2003 IEEE International Symposium on Industrial Electronics (Cat. No.03TH8692)*. Vol. 2. 2003, 821–825 vol. 2. DOI: 10.1109/ISIE.2003.1267926.

[21] N. S. Gameiro and A. J. M. Cardoso. "A New Method for Power Converter Fault Diagnosis in SRM Drives." In: *IEEE Transactions on Industry Applications* 48.2 (2012), pp. 653–662. ISSN: 0093-9994. DOI: 10.1109/TIA.2011.2180876.

[22] K. Lu. "A new fault-tolerant switched reluctance motor with reliable fault detection capability." In: *2014 17th International Conference on Electrical Machines and Systems (ICEMS)*. 2014, pp. 1881–1886. DOI: 10.1109/ICEMS.2014.7013790.

[23] S. Mir, M. S. Islam, T. Sebastian, and I. Husain. "Fault-tolerant switched reluctance motor drive using adaptive fuzzy logic controller." In: *IEEE International Electric Machines and Drives Conference, 2003. IEMDC'03.* Vol. 2. 2003, 835–841 vol.2. DOI: 10.1109/IEMDC.2003.1210332.

[24] N. S. Gameiro and A. J. M. Cardoso. "Fault tolerant power converter for switched reluctance drives." In: *2008 18th International Conference on Electrical Machines*. 2008, pp. 1–6. DOI: 10.1109/ICELMACH.2008.4800210.

[25] J. Borecki and B. Orlik. "Fault-tolerant, multilevel converter topology for switched reluctance machines." In: *2017 19th European Conference on Power Electronics and Applications (EPE'17 ECCE Europe)*. 2017, P.1–P.10. DOI: 10.23919/EPE17ECCEEurope.2017.8099205.

[26] Q. Sun, J. Wu, C. Gan, and J. Guo. "Modular Full-Bridge Converter for Three-Phase Switched Reluctance Motors With Integrated Fault-Tolerance Capability." In: *IEEE Transactions on Power Electronics* 34.3 (2019), pp. 2622–2634. ISSN: 0885-8993. DOI: 10.1109/TPEL.2018.2846539.

[27] Z. Qing, G. XiBin, G. YaJing, D. Lei, and W. HongXing. "Design of double redundancy switched reluctance motor." In: *2017 Chinese Automation Congress (CAC)*. 2017, pp. 7482–7486. DOI: 10.1109/CAC.2017.8244131.

[28] M. Ruba, L. Szabo, L. Strete, and I. Viorel. "Study on fault tolerant switched reluctance machines." In: *2008 18th International Conference on Electrical Machines*. 2008, pp. 1–6. DOI: 10.1109/ICELMACH.2008.4799994.

[29] M Becheikh, Y. Messlem, and B. Azeddine. "An 8/6 Switched Reluctance Motor Calculations Using a Combined FE-BE Methods." In: (Oct. 2008).

[30] F. Soares and P. J. Costa Branco. "Simulation of a 6/4 switched reluctance motor based on Matlab/Simulink environment." In: *IEEE Transactions on Aerospace and Electronic Systems* 37.3 (2001), pp. 989–1009. ISSN: 0018-9251. DOI: 10.1109/7.953252.

[31] W. Ding, Y. Hu, and L. Wu. "Investigation and Experimental Test of Fault-Tolerant Operation of a Mutually Coupled Dual Three-Phase SRM Drive Under Faulty Conditions." In: *IEEE Transactions on Power Electronics* 30.12 (2015), pp. 6857–6872. ISSN: 0885-8993. DOI: 10.1109/TPEL.2015.2389258.